Sakari Lapinsuo

Thin Film Coatings by Atomic Layer Deposition for Improvement of the Flexural Strength of Glass

School of Electrical Engineering

Thesis submitted for examination for the degree of Master of Science in Technology.

Helsinki 27.5.2013

Thesis supervisor:

Prof. Ilkka Tittonen

Thesis instructor:

Lic.Sc. (Tech.) Olli Jylhä

Aalto University
School of Electrical
Engineering

AALTO UNIVERSITY
SCHOOL OF ELECTRICAL ENGINEERING

ABSTRACT OF THE
MASTER'S THESIS

Author: Sakari Lapinsuo

Title: Thin Film Coatings by Atomic Layer Deposition for Improvement of the Flexural Strength of Glass

Date: 27.5.2013 Language: English Number of pages:7+63

Department of Micro and Nanotechnology

Professorship: Micro- and Nanosystems Code: S-129

Supervisor: Prof. Ilkka Tittonen

Instructor: Lic.Sc. (Tech.) Olli Jylhä

This work is a study of glass strengthening by atomic layer deposition (ALD) conducted at the cleanroom facilities of Beneq Oy in Espoo, Finland. Optimization of ALD process parameters was preceded by an investigation of best practices for testing glass, including but not limited to cutting, washing, lamination, and flexural testing (including reliability analysis) of glass.

Glass substrates were encapsulated primarily with Al_2O_3 films using trimethylaluminum (TMA) and H_2O as precursors. The effect of film thickness (between 5-100nm) and reaction temperature (100-475°C) on glass strength was studied by standardized bending tests. Film thickness and uniformity were verified by ellipsometry.

The results indicated that atomic layer deposition, partly due to its reliability, repeatability, and layer thickness conformity even in large batches can be used to strengthen glass for industrial scale applications. The amount of improvement in strength is largely dependent on the type of glass and its pre-ALD treatment. While little improvement was achieved with chemically strengthened glass, glass without chemical strengthening showed in most cases very good or at least significant improvement depending on the applied test method, type of glass and the meter used for comparison.

Keywords: ALD, atomic layer deposition, glass, strengthening, reinforcement, aluminum oxide, Al_2O_3, ball-on-ring, BOR, bending test, flexural strength

AALTO-YLIOPISTO
SÄHKÖTEKNIIKAN KORKEAKOULU

DIPLOMITYÖN
TIIVISTELMÄ

Tekijä: Sakari Lapinsuo

Työn nimi: Atomikerroskasvatuksella valmistettujen ohutkalvopinnoitteiden käyttö lasin taivutuslujuuden parantamisessa

Päivämäärä: 27.5.2013 Kieli: Englanti Sivumäärä:7+63

Mikro- ja nanotekniikan laitos

Professuuri: Mikro- ja nanosysteemit Koodi: S-129

Valvoja: Prof. Ilkka Tittonen

Ohjaaja: TkL Olli Jylhä

Tämä työ käsittelee Beneq Oy:n Espoon puhdastiloissa tehtyä tutkimusta lasin vahvistamisesta atomikerroskasvatusmenetelmällä. Ohutkalvojen kasvatuksen optimointia edelsi selvitys parhaista toimintatavoista lasin lujuuden testaamisessa, johon liittyy mm. lasin leikkaaminen, peseminen, laminointi, ja taivutuslujuuden selvittäminen (ml. luotettavuusanalyysi).

Erityyppisten lasikappaleiden pinnoille kasvatettiin pääasiassa trimetyylialumiinista (TMA) ja vedestä tehtyä alumiinioksidia (Al_2O_3). Ohutkalvojen paksuuden (5-100nm) sekä niiden kasvatusprosessilämpötilan (100-475°C) vaikutusta lasin lujuuteen tutkittiin standardoiduilla taivutuskokeilla. Kalvojen paksuudet ja niiden konformaalisuus mitattiin ellipsometrilla.

Tutkimuksen tulokset osoittivat, että atomikerroskasvatusta voidaan käyttää lasin vahvistuksessa teollisessakin mittakaavassa mm. sen luotettavuuden, toistettavuuden, ja ohutkalvon konformaalisuuden ansiosta. Vahvistuksen määrä riippuu pitkälti lasityypistä ja lasin esikäsittelystä. Kemiallisesti vahvistettua lasia saatiin vahvistettua vain jonkin verran, mutta sen sijaan kemiallisesti vahvistamaton lasi vahvistui entisestään suurimmassa osassa tapauksia vähintäänkin merkittävästi, riippuen testausmenetelmästä, lasityypistä, ja vertailumittarista.

Avainsanat: ALD, lasi, vahvistaminen, alumiinioksidi, Al_2O_3, ball-on-ring, BOR, taivutustesti, taivutuslujuus

Preface

The research presented in this thesis has been carried out at the Beneq Oy cleanroom facilities located at Espoo, Finland between January and December 2012.
I would like to express my appreciation for Mr. Sampo Ahonen and Mr. Sami Sneck for recruiting me for Beneq Oy in January 2012. I would also like to thank Prof. Ilkka Tittonen for supervising my work.

Many thanks go to my instructor Lic.Sc. (Tech) Olli Jylhä for the professionalism and personal encouragement he has provided not only with the practical work but also with theoretical analysis and strategic thinking. The resources he has provided through communication with many glass and mobile device manufacturers and of course the ALD group at Beneq Oy has been invaluable.

I also highly appreciate the help, expertise and fellowship of my other contemporaries at Beneq Oy (or former Planar Oy): Tapani Alasaarela, Jonas Andersson, Markus Bosund, Jouni Hujakka, Markku Kääriä, Hannu Leskinen, Jarmo Maula, Milja Mäkelä, Matti Putkonen, Pekka J. Soininen, Martti Sonninen, and Tero Taipale. Further, I feel grateful for the interest and encouragement I have received from my friends, especially within the LDS church.

Finally, my deepest thanks go to my parents and the rest of my family, and first and foremost to my Creator, for their loving support throughout my studies.

Helsinki, 19.4.2013

Sakari Lapinsuo

Contents

Symbols and acronyms

Symbols

σ	stress
T	temperature
E	Young's modulus
μ	Poisson's ratio
Y	non-dimensional crack shape factor
K_{IC}	glass toughness
c	crack depth
x_c	depth-of-layer (DOL)
t	ALD coating thickness
η	viscosity
α	coefficient of linear thermal expansion
L	separation between supporting edges in 3- and 4-point flexural tests
l	separation between loading edges in 3- and 4-point flexural tests
P_{fi}	i^{th} ranked data point of strength σ_{fi}
N	total number of glass articles used in one bending test set
b	width of glass specimen
h	height of glass specimen
F	failure force recorded by the materials testing machine at the time of failure
β	Weibull scale parameter or characteristic strength of the Weibull distribution
m	Weibull modulus or shape parameter of the Weibull distribution

Acronyms

4PB	four-point bending (test)
3PB	three-point bending (test)
ALD	atomic layer deposition
ALE	atomic layer epitaxy
BOR	ball-on-ring
CS	compressive stress
CTE	coefficient of thermal expansion
CVD	chemical vapor deposition
DOL	depth of layer
GPC	growth per cycle
IOX	ion exchange
ML	maximum likelihood
MRR	medium-rank regression
OLS	ordinary least squares
PTFE	polytetrafluoroethylene
SCG	slow crack growth
SLM	standard liters per minute
TMA	trimethylaluminum

1 Introduction

The rapid growth of mobile technology in the past decade has increased the interest of glass and display manufacturers to improve the strength of glass while maintaining glass' other desirable qualities such as good transparency and high scratch resistance. Chemical strengthening has been the most recent method for glass reinforcement for many high-performance mobile devices such as high-end mobile phones and tablets. However, the process requires a minimum thickness of approximately 300μm [1]. As manufacturers transition into using thinner glass, chemical strengthening might no longer be the choice technology.

The primary goal of this study is to gain a sound understanding of the mechanical equipment and methods for testing glass, and the analysis and correct interpretation of the test results. The second objective is to investigate the feasibility of using thin films grown by Atomic Layer Deposition (ALD) in order to achieve one or more of the following functions:

1) Further reinforce chemically strengthened glass for extra strength

2) Replace time-consuming and more expensive processes related to chemical strengthening

3) Introduce ALD as a novel way to strengthen ultra-thin glass (thickness less than 0.5mm)

The underlying theory behind glass strengthening by ALD is based on partially filling nano-scale cracks inherent to brittle glass. Flawless glass is very strong, in the order of several gigapascals which is the theoretical stress needed for breaking atomic bonds. However, because of interior and surface flaws, the stress needed to fracture bulk glass is only around 100 megapascals [3]. The imperfections act as initiation centers for brittle fracture. Thus, if they can be healed by changing the surface topography of glass by means of ALD, it is possible to significantly improve the strength of glass. In effect it is assumed that the dominating cause for failure is indeed surface flaws, not interior flaws.

Atomic layer deposition is known for its excellent uniformity, conformity and thickness control of the deposited thin film in the nanometer range. Aluminum oxide grown from compound reactants trimethylaluminum and distilled water was the primary depositant. This is due to the material's thermal and chemical stability, excellent dielectric properties, easy upscalability, and good adhesion to many surfaces.[4]

Efforts to optimize the ALD process for maximum improvement in strength concentrated primarily on two process variables: temperature and coating thickness. Coating thickness varied within the 5-100nm range. However, most coatings were no thicker than 30nm in order to keep optical transmission above a reasonable limit. Thicker coatings were used to aid in the discovery of coating thickness and reaction chamber temperature related trends. Film thickness and uniformity were verified by ellipsometry. Process temperature in the reaction chamber was kept between 100°C and 475°C in order to ensure the production of high quality film.

All glass used in this study was supplied by manufacturers within the display, mobile phone, and glass industry. The majority of provided samples was chemically strengthened silicate glass used as cover glass for mobile phones. Remaining test specimens were either alkali-free aluminosilicate or aluminoborosilicate glass.

The effect of film thickness and reaction temperature on the flexural strength of glass was studied using three types of tests that closely adhered to standardized bending tests: the four-point bending (4PB) test, the three-point bending (3PB) test, and the ball-on-ring (BOR) test. Of these the four-point bending test was used most frequently. It focuses on edge strength just as the three-point bending test. The ball-on-ring test was used to test the face strength of glass.

The following more business oriented questions were kept in mind during the course of this study:

1) Can the use of ALD be cost-effective?

2) Is the ALD process industrially scalable and can it be satisfactorily implemented as part of a manufacturing line?

3) How great of an improvement in flexural strength would be interesting for customers?

4) How important is the type of glass used?

5) What pre-ALD steps could be required from manufacturers (e.g. cleaning)?

6) Can ALD be combined with chemical strengthening?

7) In which part of the supply chain would the target customers be located?

In conclusion, it is important to note that the aim of this work has not been to provide direct proof for the aforementioned theory. In fact, while e.g. atomic force microscopy or similar methods could be employed before or after coating, or before or after testing, it was determined to be too difficult if not impossible at this time to investigate the crack tips to see the effect of a coating on them. Therefore, there is no guarantee that those samples that underwent significant improvement in strength are stronger exactly because the samples' surface flaws had somehow been eliminated. Limited availability of samples imposed some restrictions on the research relating to the theoretical models presented hereafter and the scale and complexity of test matrices for strength optimization.

2 Theoretical background and previous research

2.1 Introduction to Atomic Layer Deposition

What is known today as atomic layer deposition is most commonly acknowledged to have been developed under the name "atomic layer epitaxy" (ALE) in Finland by Tuomo Suntola and Jorma Antson in the 1970s for the development of semiconducting doped zinc sulfide films in electroluminescent displays [6]. A comprehensive overview and general background on the development of ALD was published by Puurunen [7].

ALD is a thin film deposition technique that is based on sequential use of self-terminating gas-solid reactions. The majority of ALD reactions use two chemicals, element or compound reactants typically called precursors. One reaction cycle consists of four characteristic steps:

1) A self-terminating reaction of the first reactant

2) A purge or evacuation to remove the nonreacted reactants and the gaseous reaction by-products

3) A self-terminating reaction of the second reactant

4) A purge or evacuation similar to step 2

The amount of material grown during one cycle is called the "growth per cycle" (GPC). This can change according to several factors such as temperature, number of reaction cycles, growth mode and type of reactants used. The ALD process is preceded by stabilization of the substrate surface to a known, controlled state - in this study by heat treatment.

Adsorption of precursors or parts of precursors can take place through physisorption and chemisorption. Physisorption originates from weak interactions whereas chemisorption involves the making and optionally breaking of chemical bonds. Adsorption can be irreversible or reversible. However, for adsorption to be self-terminating, the adsorbed material may not desorb from the surface during the purge or evacuation. As a result, in ALD the type of adsorption is limited to irreversible adsorption. This requirement of irreversibility restricts the type of adsorption to chemisorption because physisorption is always reversible.

It is often incorrectly assumed that a monolayer of the ALD-grown material should form per cycle. Because of steric hindrance of ligands (ligands of the chemisorbed first reactant shield part of the surface from being accessible to the second reactant), the GPC in ALD from compound reactants such as those used in this study should be considerably less than a monolayer. Experimental GPC values very within about 15-30% of a monolayer, depending on the growth temperature.

2.1.1 Effect of temperature on GPC

There are four characteristic ways in which GPC can depend on temperature:

1) GPC is inversely proportional to increasing temperature

2) GPC is directly proportional to increasing temperature

3) GPC stays constant with temperature (sometimes GPC settles to different constant values at different temperatures)

4) GPC may first increase and then decrease with temperature

In the first case an increase in temperature may lower the number of reactive surface sites, or, the inherent reaction mechanism changes. In the second case some energy barriers may be overcome at higher temperatures. The third case may occur if steric hindrance causes saturation and the number of reactive sites does not affect the amount of adsorbed species. The last case can be considered a combination of the first and second case. It is also possible that a lower GPC be caused by a decrease in the number of reactive sites because of incomplete reactions due to lower reaction rates and slower mass transport at lower temperatures.

Data on the effect of temperature on GPC in this study is found in the results section (4.1.2).

2.1.2 Effect of the number of cycles on GPC

A change in the chemical composition of the surface on which material is grown makes GPC vary with the number of cycles. While the first reactions occur on the substrate surface, the later reactions occur on either both the substrate and the ALD-grown material, or later on a surface with only the ALD-grown material exposed. Four groups are used for classification of ALD processes based on how the GPC varies with the number of reaction cycles:

1) Linear growth (GPC stays constant over the cycles)

2) Substrate-enhanced growth (GPC is higher in the beginning)

3) Substrate-inhibited growth, Type 1 (GPC is lower in the beginning)

4) Substrate-inhibited growth, Type 2 (similar to Type 1, but in addition GPC reaches a maximum before settling to a constant value)

2.1.3 Surface chemistry of the $AlMe_3/H_2O$ process

The $AlMe_3$(or TMA)/H_2O process is considered ideal for ALD. This is because the reactants are highly reactive, but at the same time thermally stable. In addition, the gaseous reaction product methane does not interfere with the growth. The process gives smooth, conformal films on highly complex structures. The $AlMe_3/H_2O$ process is divided into two half reactions:

$$\|Al - OH + Al(CH_3)_3(g) \rightarrow \|Al - O - Al(CH_3)_2 + CH_4(g) \quad (1)$$

$$\|Al - CH_3 + H_2O(g) \rightarrow \|Al - OH + CH_4(g) \quad (2)$$

The full reaction stoichiometry is:

$$Al(CH_3)_3(g) + \frac{3}{2}H_2O(g) \rightarrow \frac{1}{2}Al_2O_3(s) + 3CH_4(g) \quad (3)$$

The $AlMe_3/H_2O$ process is self-terminating because past a certain minimum pulse or purge length GPC does not increase with length. However, too short purges increase GPC due to incomplete washing and therefore simultaneous mixing of the two precursors, thereby enabling CVD-type deposition.[7]

2.1.4 Advantages and disadvantages of ALD

One of the greatest advantages of ALD is its excellent thickness control, a fact that presents itself also through this study. This is because film thickness depends only on the number of reaction cycles. Unlike with CVD, there is less need for reactant flux homogeneity. Coatings can be applied on objects with large and complex surface areas. The process can be upscaled with excellent reproducibility and conformity. The latter is especially important in this application because glass always breaks at its weakest point. It is important to be secure that a grown film is as thick and dense as it was meant to be at any given location on a coated surface.

Growth of different multilayer structures is straightforward with ALD. Wide range of film materials can be used, and the grown layers have high densities with low impurity levels. One significant advantage is also the possibility to use lower deposition temperatures. This property proved to be especially useful in this work because chemically strengthened glass was shown to lose some of its strength if exposed to temperatures above a certain limit over an extended period of time.

The most important disadvantage of ALD is its relative slowness. However, in this study a large batch size due to the small size of samples compensated for slowness. Also, the coating process itself (excluding pre-heating) was not long as the layer thickness was kept under 100nm.

2.2 Introduction to the nature of glass

In science the term *glass* often includes every solid that possesses a non-crystalline (i.e. amorphous) structure and that exhibits a glass transition when heated towards the liquid state. Even polymer glasses such as acrylic glass and polycarbonate are included within this definition.[9]

In this study, however, the definition is more confined. The glass used in this work can be categorized as technical glass. Such glass has had a major influence on the development of important technological fields such as chemistry, pharmaceutics, automotive, optoelectronics and renewable energy. Vice versa, traditional areas of technical application for glass such as laboratory apparatus, flat panel displays and optoelectronics led to the development of a great variety of special glass types and new forming processes.

Technical glasses can roughly be arranged in the following four groups, according to their oxide composition (in weight percent).[8]

1) Borosilicate glasses that contain substantial amount of silica (SiO_2) and boric oxide (B_2O_3>8%) as glass network formers; the amount of boric oxide affects the glass properties such as chemical resistance

2) Alkaline-earth aluminosilicate glasses which are free of alkali oxides and contain 15-25% Al_2O_3, 52-60% SiO_2, and about 15% alkaline earths

3) Alkali-lead silicate glasses which typically contain over 10% lead oxide (PbO)

4) Alkali alkaline-earth silicate glasses, better known as soda-lime glasses, that contain about 15% alkali (usually Na_2O), 13-16% alkaline earths (CaO + MgO), 0-2% Al_2O_3 and about 71% SiO_2

The glass samples used in this study were either from the first or fourth category. The different qualities possessed by different types of glass depend upon their chemical makeup and method of production. The properties can be divided into five categories: chemical, mechanical, thermal, electrical and optical properties.

2.2.1 Chemical resistance of glass

In terms of chemical resistance, glass is superior to most metals and plastics. It is highly resistant to water, salt solutions, acids, and organic substances. Especially at high temperatures glass is significantly vulnerable only to hydrofluoric acid, strong alkaline solutions, and concentrated phosphoric acid. Every chemical attack on glass involves water or its dissociation product, i.e. H^+ or OH^- ions. These ions replace the easily soluble glass components on the surface, forming a so-called silica-gel layer which often proves to be more resistant than the base glass. With prolonged exposure the layer becomes thicker and opaque, and finally peels of, rendering the glass useless for any application.

Between the stages of initial wear and total ablation there is a wide scope of possible surface modifications, some of which, although optically visible, are of no practical significance. For less resistant glasses even small amounts of water (air moisture and condensation) in the presence of other agents such as carbon dioxide or sulfur oxides can lead to surface damage. Hand perspiration or impurities left by detergents can induce strongly adhering surface defects, mostly recognizable as stains. If the glass is afterwards reheated (>350-400°C), the contaminants or some of their components may burn in. [8]

Some of the glass used in this study was cleaned by ultrasound using deionized water and alkaline detergent. More details on glass exposure to aqueous solutions are found in the materials and methods section (3.2).

2.2.2 Mechanical and thermal properties of glass

Viscosity of a fluid is a measure of its resistance to deformation. A steady change in the viscosity in all temperature regions is a fundamental characteristic of glass (see Figure 1). Between melting temperature and room temperature, the viscosity of glass increases by 15-20 order of magnitude. Within this range, glass is subject to three different thermodynamic states:

1) Melting range (above liquidus temperature T_s; maximum temperature at which crystals can co-exist with the melt in thermodynamic equilibrium)

2) Range of supercooled melt (between liquidus temperature T_s and transformation temperature T_g, also called the annealing point)

3) Frozen-in, quasi-solid melt ("glass range"; below transformation temperature T_g)

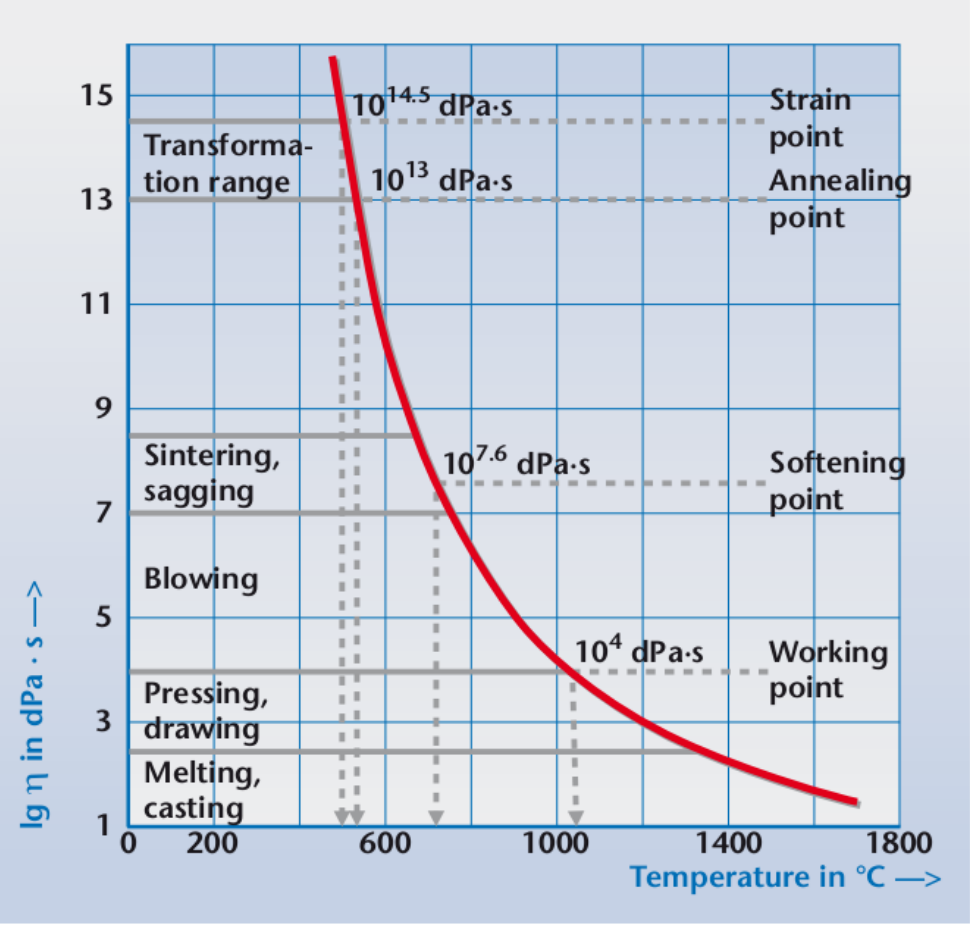

Figure 1: A typical viscosity-temperature curve. The vertical axis shows the logarithm of the viscosity η expressed as dPa·s.[8]

The upper bound of a so-called annealing range is the annealing point. The lower bound is the strain point, which lies about 30-40°C below the annealing point. Between these two points it takes different amounts of time for relaxation of internal stresses. What is important in this study is that the temperatures used in the ALD process stay well below the transformation range, or in other words below the strain point. This is in fact the case as the strain points for the glasses used in the experiments are above 500°C. The expectation therefore is that the pre-heating before thin film deposition does not affect the internal structure of the glass samples. However, this is not to dismiss the possibility of weakening of glass in the pre-heating stage. While the internal structure might stay unaffected, there is a possibility for the thermal expansion to widen or deepen the cracks inherent to the glass surface.

Another point to consider is the pre-heating effect on strengthened glass. It has been shown that thermally prestressed glasses show significant stress relaxation already at 200-300°C [8] below the transformation temperature. Similar results can be expected for chemically strengthened glass, which calls for the carrying out of heating-only tests before actual coating tests (that always include the pre-heating stage before coating).

The theoretical strength of glass ($>10^4$ MPa) is much higher than in practice due to surface defects induced by wear. These defects drop the practical tensile strength to approximately 20-200 MPa. It is important to note that according to a Schott AG's guide to technical glasses [8], the effect of the chemical composition of silicate glasses on strength is almost negligible.

Tensile strength is both time-dependent and stress rate-dependent. In stress testing, faster load rates lead to higher tensile strengths. Also, depending on the glass type, the tensile strength under constant loading (for years of loading) will only amount to about 1/2 to 1/3 of the experimental tensile strength.[8]

There is also a stressed area-dependence. The larger the stressed area is, the higher is the probability of large defects within this area. This effect must be considered when comparing test setups with different sizes of stressed areas.[8]

Interestingly the surface condition or the time or stress rate dependence do not influence the tensile strength when compressive stress is introduced to the glass surface for instance by ion exchange (IOX; 50-200µm thick compressive surface layer). This is because the compressive surface stress exceeds the externally applied tensile stress and so the surface is kept under total compressive load. In other words, by adding compressive stress to the glass, the compressive force must be overcome before the surface becomes tensile in nature (equation (4)).[8]

$$\sigma = \sigma_{y,0} + \sigma_{compressive} \tag{4}$$

Most glasses have a positive coefficient of thermal expansion α, normally between 3.3-12$\times$ 10^{-6}/K. This is an important characteristic to note when growing thin films on top of glass because the difference in the coefficients of the glass and the thin film could give rise to unadvantageous tensile stresses. Further, due to the low thermal conductivity of glass (typically 0.9-1.2 W/m(m·K) at 90°C), temperature changes produce relatively high temperature differences between the surface and the interior.

This can result in stresses defined by equation (5). Because cracks originate almost exclusively from the glass surface and are caused there by tensile stress alone, cooling processes are usually much more critical than the continuous rapid heating of glass articles.[8]

$$\sigma = \frac{\Delta T \alpha E}{1 - \mu} [\text{MPa}] \tag{5}$$

2.2.3 Electrical and optical properties of glass

When choosing a glass for electrical or electronic applications, there are several characteristics to consider. These are the volume resistivity (resistance in ohms between opposite faces of a centimeter cube of the glass tested; important when glass is used as an insulator), surface resistivity (ratio of the potential gradient parallel to the current along its surface, to the current per unit width of the surface; this method is used to measure the conductivity of coated glass), and the dielectric constant (ratio of energy stored in a condenser with the glass as the dielectric, compared with the energy stored in the same condenser with air as the dielectric; this is used to measure the ability of glass to store electrical energy). As the focus of this work was not on the electrical properties of coated glass, this field of interest was left unexplored.

The most relevant optical properties of glass are the refractive index, dispersion, transmission, reflectivity, and absorption (amount of light energy converted to heat within the glass that is not transmitted nor reflected). Of these, only the transmission of light in the visible range was of greater interest. Even then only a fraction of the samples were analyzed for transmittance. See the results section for more data (4.1.5).[2]

2.2.4 Modern production of flat glass

The float process (see Figure 2) is the modern way of producing flat glass for products such as mirrors, windows and flat-panel displays. The raw materials like silica sand, soda ash, salt cake, dolomite, limestone and feldspar are mixed and melted in a furnace before being fed through rollers into a float bath. The molten glass floats on a molten tin bed and as it moves through the bath, it is cooled down to a temperature where a certain viscosity is reached. At this viscosity level the glass is spread by gravity or by applied extra pressure to a desired thickness. It is then annealed to prevent the formation of nonuniform internal stresses. The solidified glass sheets are finally cut by first scribing a score line with a diamond tip or laser and then applying pressure to advance the crack. Flat glass produced by the float method has excellent thickness control and strength. The float method is also better suited for mass production because its effective width is greater than in the fusion method [5].[10]

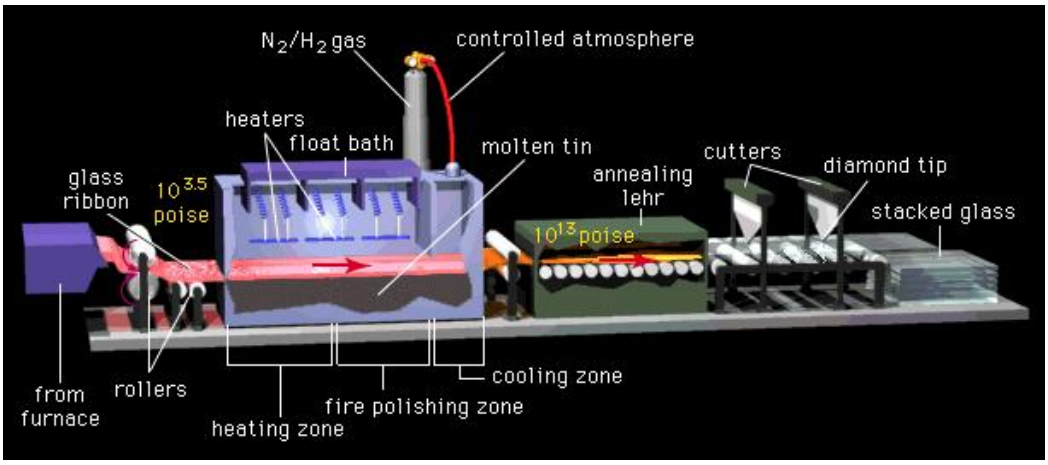

Figure 2: Schematic diagram of a float process for making flat glass.[10]

Some of the molten tin is picked up by the face of glass in contact with the tin. The small difference in the chemical makeup of the two faces of glass must therefore be considered in view of the testing process. In most experiments the glass articles were fully encapsulated by ALD so there was no need to record which side was coated. However, in testing of the flexural strength of the glass specimens, the side of sheet under tension was recorded (and chosen as instructed by the glass manufacturers or customers).

A new glass forming method (see Figure 3) known as the overflow downdraw method or the fusion method was developed by Corning Inc. in the 1960s and originally used for manufacturing automotive windshields. It was later shelved for years, but then reintroduced for other applications, including flat screens displays. The key advantage of the fusion method as compared to the float method is the exceptional thickness control and surface quality. In fact, the pristine surface quality requires no subsequent surface grinding or polishing that follow the float process [15]. Today the technique is used by many glass manufacturers for the production of TFT-LCD display devices.[11, 12, 13, 14]

2.3 Glass strengthening

Most glass breakage is due to tensile strength failure because glass is very low in tensile strength and extremely high in the amount of compressive stress it can withstand. The tensile strength can be increased by introducing compressive stress into the structure (see equation (4)). This is typically accomplished by thermal treatment (heat strengthening or heat tempering) or chemical bath (ion exchange). Heat strengthening, which does not produce a full dicing pattern when the glass is broken, is a mild form of heat tempering. Heat tempering causes some optical distortion and is appropriate for glass from a few millimeters to approximately one meter thick with sizes from 1" diameter to 48"×72". Thus, because glass thicknesses for mobile

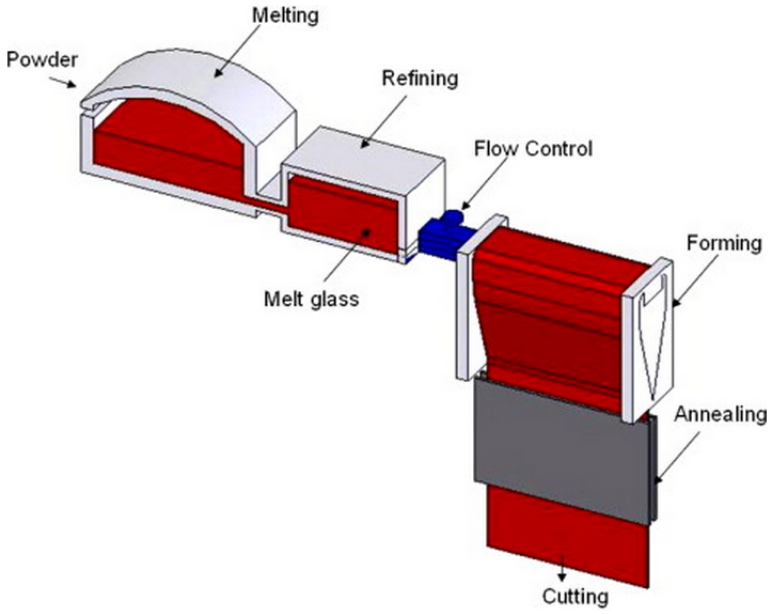

Figure 3: A schematic diagram of the overflow fusion process.[14]

displays vary from 0.5mm to 1.5mm and little or no optical change is acceptable, and because a higher surface compression (and consequently higher strengths) is achieved by chemical tempering, all strengthened glass used in this study has been chemically prestressed.[2]

2.3.1 Glass strengthening by ion exchange

Chemical strengthening provides approximately five to eight times the strength of annealed glass [2]. This is accomplished by immerging the original glass into a molten alkali salt at a temperature below the glass transition temperature. During the time of immersion, the alkali ions close to the surface of the glass and those in the alkali salt switch places without changing much of the network structure formed by the silicon-oxygen bonds in the original silicate glass. In this thermally activated inter-diffusion process glass is strengthened by an increased surface compression as long as the ions in the surrounding salt solution have a greater ionic radius than those leaving the glass.

Potassium or sodium nitrates are the most widely used salts for chemical tempering because they have low enough melting points (slightly above 300°C), and can be used safely in austenitic stainless steel tanks up to around 500°C. Keeping the ALD process temperatures in mind, it is important to note that already at 400°C nitrogen oxides are formed in the salt bath and must be released from the environment. Even if a more stable anion was used in order to enable the use of higher temperatures, chemical tempering would not become more advantageous because of viscoelastic relaxation. Thus, it is safer to assume that the temperatures used in chemical tempering stay below 400°C and that, if so, the ALD process must be

optimized so as to avoid the use of too high temperatures (too close to the salt bath temperature) that would at least partly annul the positive chemical strengthening effect.

The degree of chemical tempering is measured by the magnitude of compressive stress (CS) and the depth of the compressive stress layer (DOL, depth-of-layer). These are affected by three process parameters: bathing time, bathing temperature and the composition of the salt bath. Using higher temperatures and longer bathing times results in higher DOLs, but this comes with a compromise because at the same time the compressive strength drops due to the tendency of glass to relax some of the stress. In other words, two opposite effects have to be taken into account in the optimization of the chemical tempering process. If one wants a very high strength surface, then low temperatures should be used. In this case, however, the DOL will be shallower and any cracks that are deeper than the DOL will make the strength fall down to the level of the untreated glass. This is to say that glasses with initial surface cracks deeper than the case depth are hardly reinforced. If one knows of the possibility for deeper cracks, then a large case depth has to be favored at the cost of a lesser strength because of a lower compressive stress at the surface.

Typical surface cracks of industrial float glass have a depth of the order of 10µm [16]. Fusion drawn glass is expected to have even more shallow crack depths. In any case, the DOL of chemically strengthened technical glasses is typically well above 10µm. It is important to understand that, for example, in a glass with a surface CS of 750 MPa with a DOL of 50µm, the CS decreases at the rate of 15 MPa/µm. In effect, any polishing will reduce the surface CS and make the glass weaker.[17]

Glass strength is not an intrinsic property of glass with a fixed value. In general there is a statistical distribution of strengths, which reflects the statistical distribution of the depth of the impairing surface flaws. The calculation of the strengthening effect of chemical tempering is rather complicated, but with a simplifying assumption that the surface compression linearly decreases from σ_s down to zero at the x_c (DOL) depth, the strength σ of a glass whose most severe surface crack has a depth of c is given by equation (6).[16]

$$\sigma = Y\frac{K_{IC}}{\sqrt{\pi c}} + \sigma_s(1 - \frac{2c}{\pi x_c}) \tag{6}$$

Here Y is a non-dimensional crack shape factor and K_{IC} is the glass toughness. Note that the second term denotes the strengthening effect, and if x_c is close to c, there is no strengthening effect.

All silicate glasses can be strengthened by ion exchange if they have enough alkalis in their composition. However, there is a limit to how much alkali content can be added because alkalis lower the temperature at which viscoelastic relaxation occurs, which is undesirable. High alumina content of the glass substrate is beneficial when associated with alkali because it has been shown to reduce the number of non-bridging oxygen atoms in the silicate network, which makes the alkali diffusion coefficients larger.[16]

2.3.2 Factors affecting glass strength

Below is a list of several factors that were, through practical testing, shown to affect the strength of glass. These are discussed in more detail in the results section.

1) Cutting of flat glass to sample size
2) ALD thin film layer thickness
3) ALD process temperature
4) Friction between the materials testing machine and the samples
5) Cleaning (washing) of glass articles before the ALD process

2.4 Previous research

The excellent properties of ALD coatings led to the formation of a theory for glass strengthening. It was anticipated that when coating glass with ALD, the resulting thin film would cover the walls of the nano-scale cracks in addition to covering the flat, flawless parts of the surface. The crack tips would be smoothened (see Figures 4 and 5) and the tip radius increased. Basic fracture mechanics dictate that an increase in the tip radius leads to decreased local stress at the tip, thereby increasing the material's ability to resist cracking.

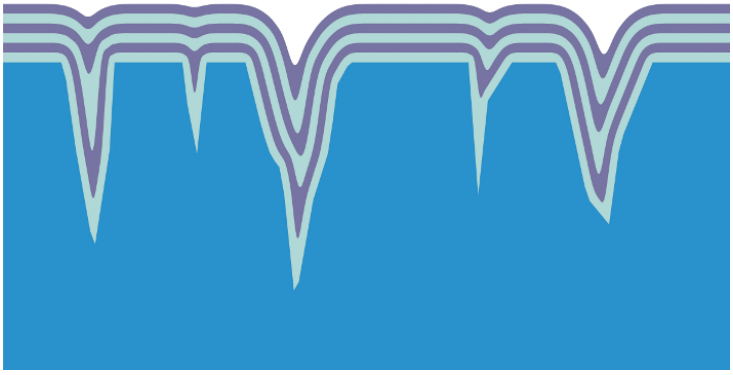

Figure 4: The original glass surface (blue) is intrinsically covered with minute cracks and imperfections called Griffith flaws. A Griffith flaw acts as a point-of-origin stress concentrator for initiating fracture. ALD technology enables the creation of invisible and durable thin film that fills the cracks and improves the crack resistance. Copyright Beneq Oy.[18]

Motivation behind this work lies in preliminary glass strengthening tests conducted in 2011. The tests showed that ALD can be effective in improving the four-point bending strength of several types of flat glass. Figure 6 shows the results

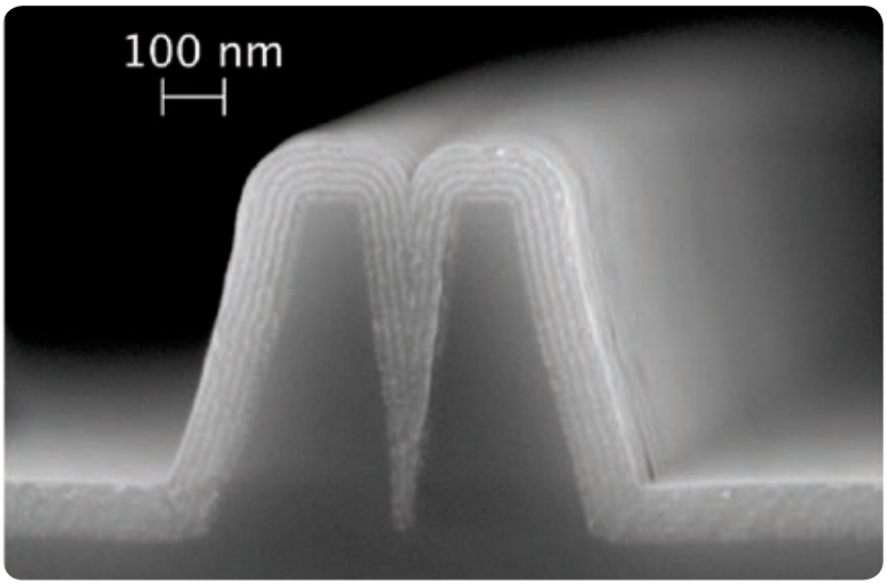

Figure 5: An artificial trench filled with an ALD nanolaminate. Image courtesy of Aalto University.[18]

of flexural strength measurements for 0.5mm thick boroaluminosilicate LCD glass, 0.7mm thick aluminosilicate touch screen glass and 0.7mm thick soda-lime silicate flat glass. The y-axis depicts the B10 failure force at which 10% of the samples fracture.[18]

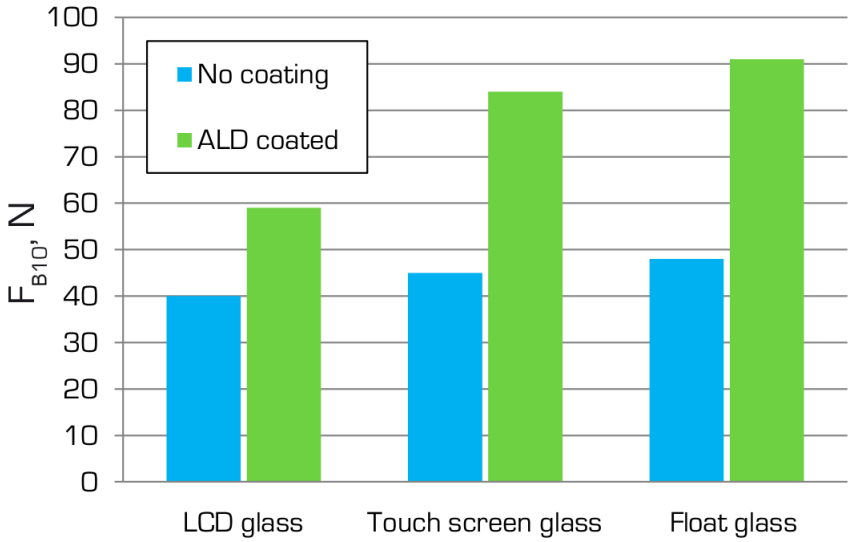

Figure 6: Results of 4-point bending flexural strength measurements by Beneq Oy for different types of flat glass. Copyright Beneq Oy.[18]

As noted earlier, it was the second objective of this work to continue the ap-

plication of ALD coatings to different types of glass articles in order to gain more understanding and proof of the ALD glass strengthening theory. The materials and methods used for this purpose are presented in the following section, followed by the results of the flexural strength tests.

3 Materials and methods

3.1 Cutting of glass

The LCD aluminosilicate float glass without chemical strengthening was the only glass type that was cut into appropriate test size from a mother glass. The glass scriber was a Kawaguchiko SS-451CP shown in Figure 7. A 3mm diameter tungsten carbide roller cutter at a 120 degree blade angle was used to scribe the glass that was placed on a vacuum chuck table. By default, glass was scribed on the side that was to be placed under tension in the bending tests. In case the glass had an anti-splinter film on it (see 3.5.1), snapping apart was followed by carefully cutting the film with a surgical knife. All pieces on which snapping produced uneven edges were discarded.

Figure 7: Kawaguchiko SS-451CP glass scriber.[30]

All chemically strengthened glass was tested in its original shape. This is because the presence of the chemically induced compressive surface layer makes conventional mechanical and even laser cutting of the ion-exchanged glass difficult or even impossible. The increased effort demanded for cutting this type of glass can lead to contamination from edge chips, resulting in weakened edges. Abramov et al.[28] describe a novel laser cutting method by which almost a flaw-free edge was achieved by optimization of the laser cutting parameters and ion exchange conditions. Using this method edge strength values reached over 500 MPa, which corresponds to flaws that are on the order of 1-5 microns.

Cutting quality was optimized with test pieces at the beginning of each cutting session, and later during cutting. The smoothness of score lines was evaluated under an optical microscope by random sampling. Figure 8 shows one such image of a cross-section of an edge of glass with a score line on its surface.

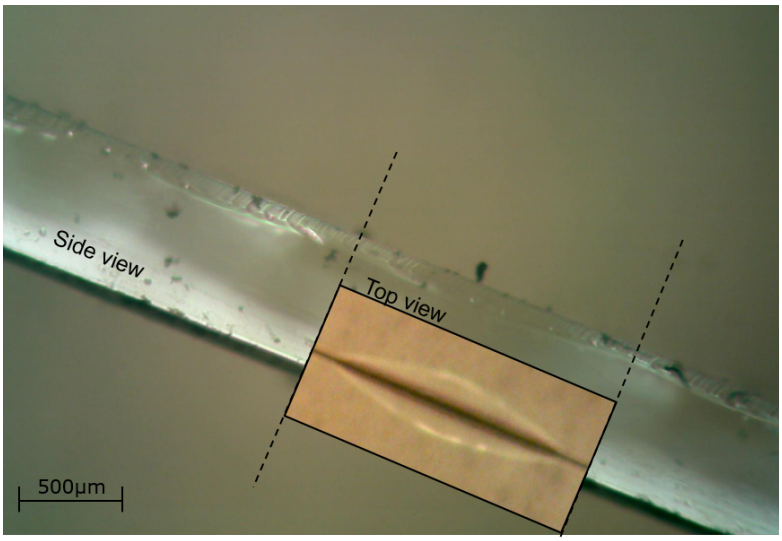

Figure 8: Image of a cross-section of a cut scribed using excessive pressure that results in unwanted oscillations. The oscillations are seen on the top of the glass in the side view and extend over 100 micrometers deep. The top view that lies over the side view depicts and is aligned with one of the oscillations in the side view. In the top view one can see that the scribe line is not clean: part of the glass on the surface has been cut off on both sides.

3.2 Washing of glass before the ALD process

Some of the alkali-free aluminosilicate LCD glass tested was machine-washed using a nylon brush and Merck Extran MA01 alkaline cleaning solution, followed by centrifugal drying. Uncoated, unwashed glass used as reference was compared with uncoated, washed glass to see weather washing had any effect on the flexural strength of glass. Similarly, both unwashed and washed glass articles were coated and tested in order to see if washing improved the flexural strength indirectly through an improved coating process.

Some of the chemically strengthened glass was also washed using a custom specified ultrasonic cleaning process consisting of several phases with pre-rinsing and post-rinsing in deionized water, and washing in between in a Merck Extran MA01 2% alkaline solution. Drying took place in a 60°C drying cabinet for at least ten minutes.

3.3 ALD equipment

Film growth was carried out with a Beneq P400 ALD system (see Figure 9). The P400 is an ideal tool for scaling-up thin film deposition from R&D phase to full-size industrial production. The P400 used in this study had been in continuous use for over two decades. It is highly reliable, industrially proven and mature in terms of technical distinction. The P400 has a commonly used flow type ALD reactor that minimizes pulse and purge times, and maximizes the precursor utilization efficiency.[20]

The coating process was preceded by careful examination of the glass articles (large

Figure 9: Beneq P800 ALD tool with an 800mm vacuum chamber diameter. The P400A is a smaller version (400mm vacuum chamber diameter) of this tool. Copyright Beneq Oy.[20]

batches by random sampling) under an inspection lamp. The glass was checked for any unwanted residue from the packaging materials (see Figure 10). For glass that was not washed at Beneq, loose particles were attempted to be removed by blowing with dry N_2.

The ALD process temperatures ranged from 100°C to 475°C. All samples were pre-heated inside the ALD chamber in vacuum and with N_2 flow for approximately four to eight hours (depending on the target temperature) before the actual coating process was started. The pressure inside the vacuum chamber was kept at 1.29±0.045 Torr (172±6 Pa), and inside the reaction chamber at 0.8±0.001 Torr (107±0.13 Pa) throughout the process. Inert N_2 gas was used as the carrier gas for transportation of precursor vapors through the reaction chamber. The flow rate was kept constant at 2.5 standard liters per minute (SLM).

The glass samples were placed on multiple trays stacked on top of each other with adequate spacing in between to ensure sufficient gas flow (see Figure 12). The stack was placed inside the reaction chamber, which was then placed in vacuum inside the ALD chamber. In most cases the reaction chamber was removed from inside the ALD chamber immediately following the completion of a coating process. This was done to minimize the possible negative effects of heating on chemically strengthened glass. However, if the process temperature was low (e.g. 100°C), the reaction chamber was sometimes left inside the vacuum chamber overnight. With high temperatures above 350°C the temperature was allowed to first drop inside the vacuum chamber before taking it out to cool (see Figure 11). This is done to prevent too steep a cooling gradient.

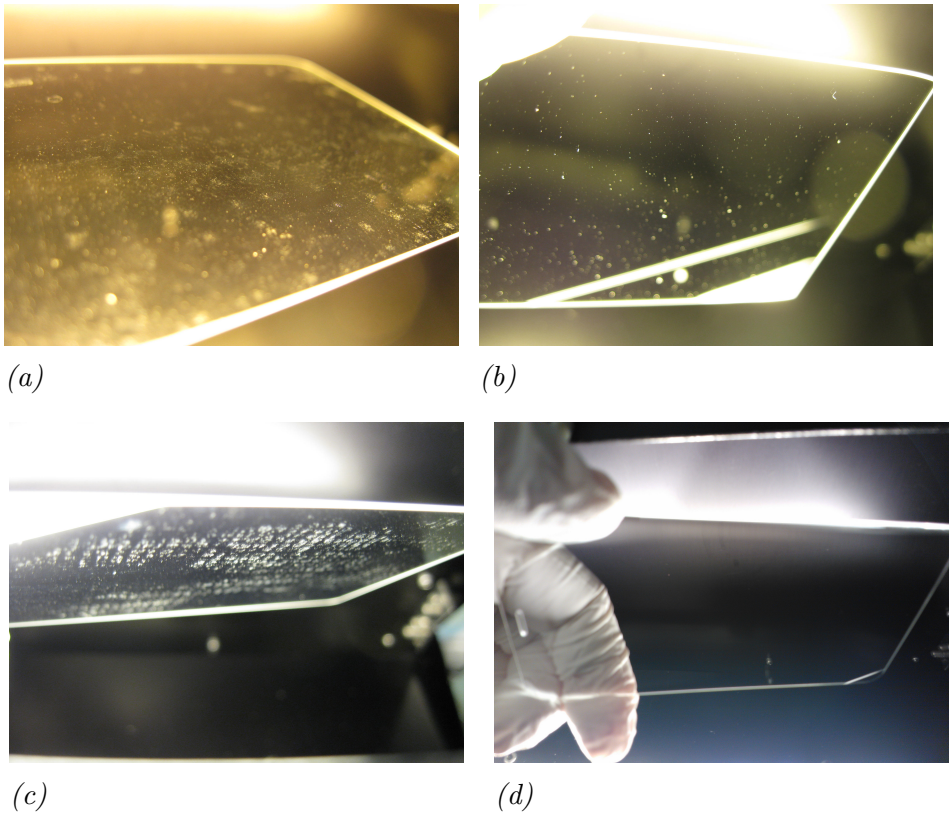

Figure 10: Glass articles from four different customers. Sample (a) suffers from insufficient cleaning while sample (b) has foreign microparticles on its surface (source unknown). The sample in subfigure (c) shows residue from impractical packaging material. Excellent vacuum packing in sample (d) leaves the glass ultraclean.

Figure 11: The P400A ALD tool with a reaction chamber in loading position. Copyright Beneq Oy.[20]

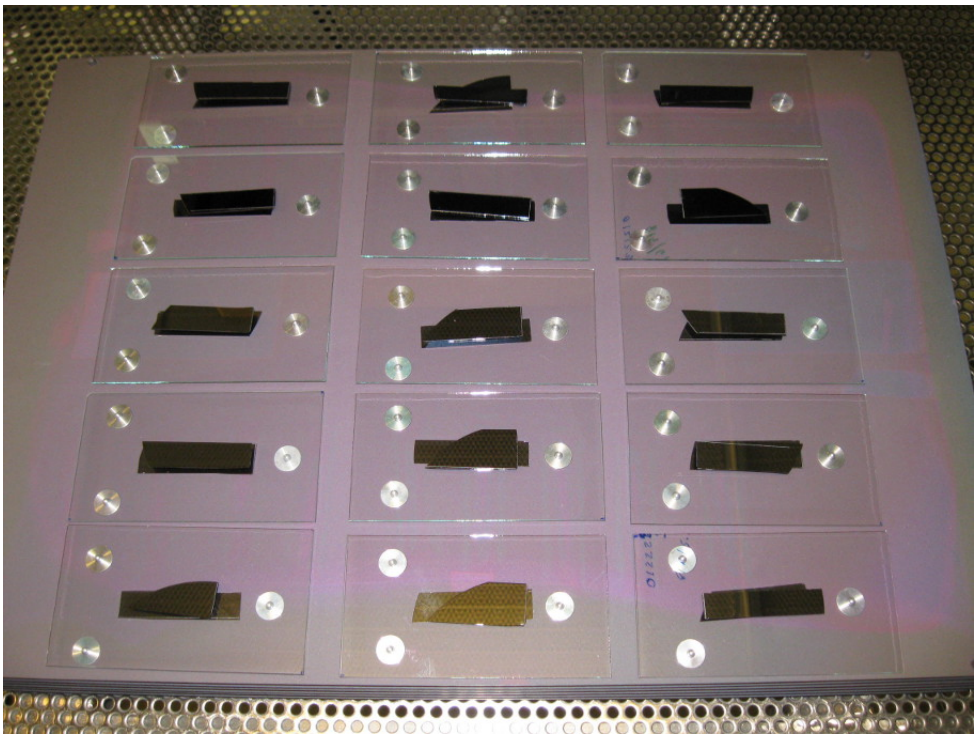

Figure 12: Glass samples aligned on one tray in a stack of trays that is placed inside the reaction chamber. The unusually high number of silicon pieces are used to verify sufficient growth uniformity in this test run prior to an actual coating process.[20]

3.4 ALD layer thickness verification by ellipsometry

For each process run, the layer thickness was measured from several silicon monitor pieces (see Figure 13) placed at various strategic locations within the reaction chamber. The number of silicon monitors depended on a few parameters such as the number of samples and the number of shelves placed in the reaction chamber.

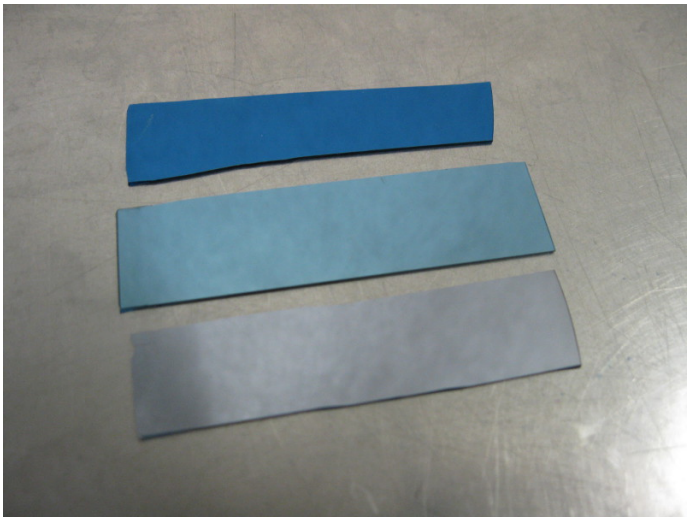

Figure 13: Visual inspection of the silicon monitors prior to ellipsometry gives an estimate of the coating thickness.

Thickness measurements were initially performed at Micronova (Aalto University) with a Plasmos SD2300 ellipsometer that uses the rotating analyzer method with a 632.8nm wavelength He-Ne laser. The measurements were carried out using a fixed refractive index of 1.6500 for Al_2O_3. The estimated thickness and refractive index of the native oxide layer on the silicon monitors was estimated to be 1.74nm and 1.46 respectively.

Later measurements were carried out in the Beneq Olarinluoma cleanroom using a Sentech SE400 advanced ellipsometer (Figure 14). Most of these measurements were performed in float mode. The laser type and method of analysis coincided with those of the Plasmos SD2300, giving both the thickness and the refractive index as a result of the measurement.

The results of the ellipsometry measurements were analyzed and used to optimize later ALD experiments. The calculated average layer thickness was used to adjust the cycle count (increase accuracy) for future processes. The calculated deviation from this average (see equation (7)) combined with the location information of the silicon monitors was used to, if necessary, relocate the glass articles to ensure uniform layer thickness (high precision) between all samples.

$$t_{deviation} = \frac{\left(\frac{t_{max} - t_{min}}{t_{ave}}\right)}{2} \cdot 100\ [\%] \tag{7}$$

Figure 14: Sentech Instruments SE400advanced ellipsometer.[19]

3.5 Materials testing machine

The apparatus used in all flexural strength tests was a Lloyd Instruments LR5K Plus 5kN materials testing machine (see Figure 15). In most tests, a 5kN loadcell with 0.5% accuracy was attached. The force measuring system exceeds the requirements of BSEN ISO 7500-1:2004, ANSI C12.20 class 0.5, ASTM E4, and DIN 1221. The crosshead speed accuracy is $\pm 0.2\%$ and the internal extension resolution better than one micron. The stiffness of the frame without the load cell is greater than 25kN/mm. Machine stiffness compensation up to 2500kN was used in all measurements although this function does not have an effect on the maximum failure force (data acquired from a stiffness compensation procedure is only used to mathematically correct the recorded extensions).

3.5.1 Test setups and standards

Three different, custom built bending fixtures or jigs were used depending on the test type (3- or 4-point bending, or BOR fixture). Figure 16a shows the ball-on-ring setup and 16b the four-point bending setup. A 0.05mm thick anti-splinter film (3M 8150M Scotchcal ClearView Graphic Film) was placed on the top surface (the side under compression) of most specimens tested for subsequent failure mode analysis. In addition, in some of the tests a PTFE foil was placed under and on top of the glass specimen in order to investigate the effect of friction on failure force. Stopper jigs were always used to ensure correct alignment of the specimens. In the case of aluminosilicate float glass, the side under tension was the air side by default. Some tests were performed to see if there was a difference in flexural strength between the air and tin sides.

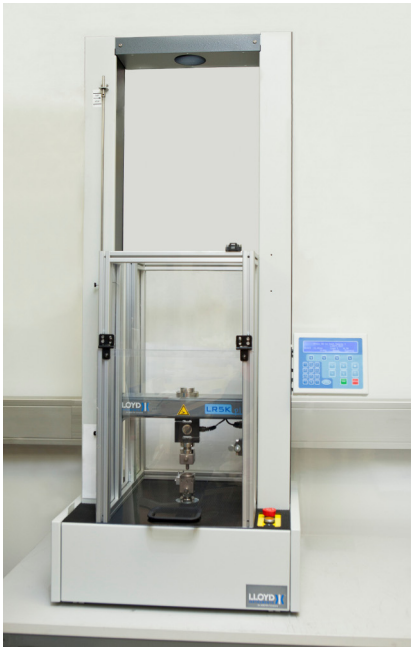

Figure 15: Lloyd Instruments LR5K Plus materials testing machine.[21]

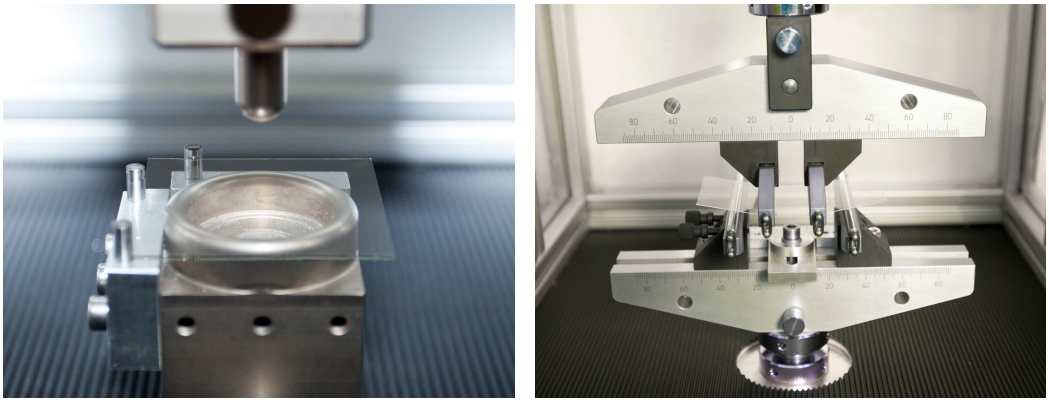

(a) *(b)*

Figure 16: Ball-on-ring (a) and four-point bending (b) fixtures. Stoppers seen in the ball-on-ring setup were adjusted according to the dimensions of the glass specimen.

All three-point and four-point bending tests were performed in accordance to Method B of the ASTM C158-02(2007) standard [31] with the following exceptions:

1) Relative humidity of the laboratory was approximately 55% (section 3.1.4)

2) The use of a controlled abrasion of the specimen as a final normalizing procedure was not implemented (section 4.5)

3) Longitudinal edges on the face to be placed in tension were not always chamfered or rounded (section 11.1.1)

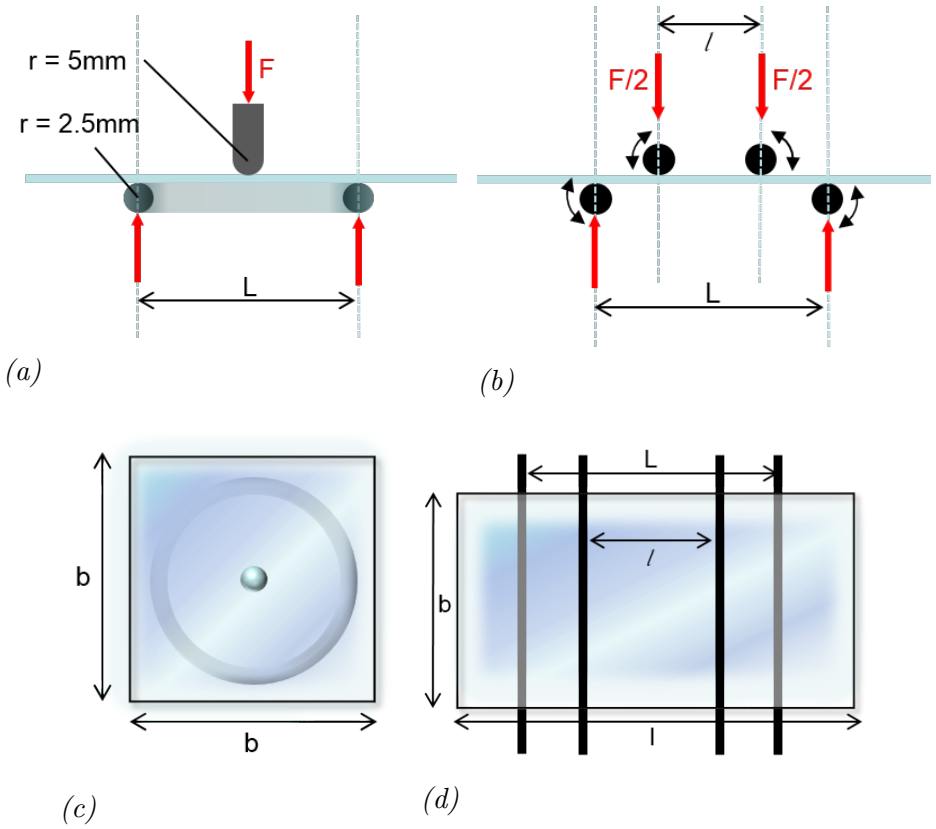

Figure 17: Side and top views of the ball-on-ring and four-point bending test setup schematics for LCD glass.

4) The width to thickness ratio for all glass articles did not fall between 2:1 and 10:1 (section 11.1.1)

5) Glass articles of rectangular form that were not prestressed (chemically strengthened) were assumed to have a degree of tensile residual stress at the midplane less than 1.38 MPa and compressive stress at the surface less than 2.76 MPa (section 3.2.2). No specimens were examined for residual stress (section 11.3.2).

6) The moment arm or separation of adjacent support and loading edges was not greater than the width of the specimen (section 12.1)

7) Point of failure as edge or face origin was recorded for only a fraction of the test specimens (section 13.2)

8) The rate of loading for both non-prestressed and prestressed glass was not determined in MPa/s. Instead, the rate was always kept between 1-5mm/min, as requested by the customers (section 13.2)

9) Number of test specimens for one test was seldom as high as 30 (section 11.2.1)

Ball-on-ring test procedures did not follow closely the practices of any one standard. However, some recommendations were adopted from standards ASTM C1499-05 [22] and BS EN 1288-5:2000 [23]. In any case all test procedures were approved by the customers prior to testing.

3.6 Fractographic analysis

Fractography is a powerful tool for analyzing fractured glasses and ceramics. It can help identify the cause of failure and even provide quantitative information about the loading conditions mainly through pattern recognition. In this study general observation about fragmentation patterns was sufficient for a diagnosis. The origin of fracture was determined to ensure that in three-point and four-point bending tests the fractures initiated from the edges and not from the faces, and vice versa in ball-on-ring tests. This information was also used to avoid misalignment of the test specimens: if the origin of fracture was clearly biased to one edge over another, then the jigs did not distribute the applied force evenly. Origin of failure was determined by visual examination of those samples that were laminated with an anti-splinter film (see Figure 18 and Figure 19).

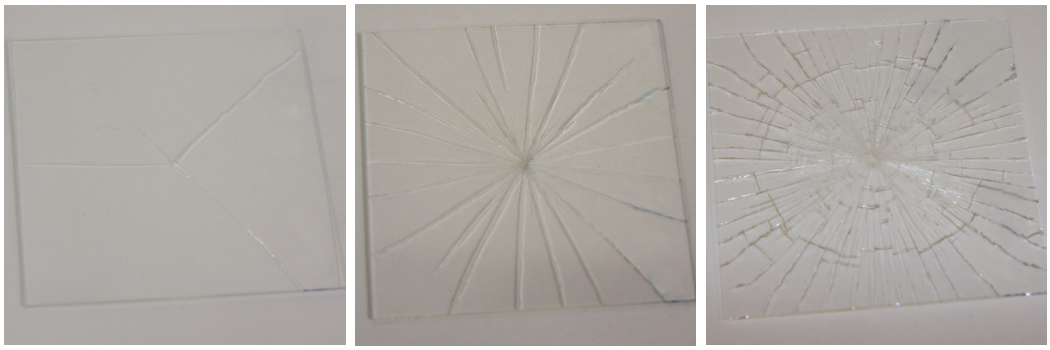

(a) 20N *(b) 120N* *(c) 500N*

Figure 18: Indications of the magnitude of the failure force are seen in the number of radial cracks. In moderate to high force failures circumferential cracking occurs, here visible in subfigure (c).

As the terminal velocity of cracks in soda lime glass is about 1500 meters per second [24], it takes only 20µs to propagate 3cm, which was the approximate distance of propagation for the glass specimens. Therefore, slow motion video recording was not possible because such a fast rate of propagation requires the use of extremely high-speed cameras that record hundreds of thousands of frames per second. Chemically strengthened glass is expected to have even greater speeds of crack propagation.

It is important to remember that even though sample dimensions is accounted for in the equations used to calculate failure stresses, the larger the test specimen (or the area under tension) is, the more likely it is to contain a severe flaw. Thus, strength varies inversely with specimen size. It is possible to scale strengths using effective volumes or surfaces. However, such scaling depends on critical assumptions. For instance, scaling cannot be done if fractography cannot confirm that the strength

(a) Low force failure *(b) High force failure*

Figure 19: For lower force failures the point of origin on the top edge is easy to locate (a). With high force failures of chemically strengthened glass it becomes more difficult (b).

limiting flaws are volume-distributed evenly. For this reason, sample size was kept constant within samples from one customer or glass type.[24]

3.6.1 Small crack growth

Many glasses are susceptible to environmentally-assisted slow crack growth (SCG). Water (or other polar molecules) as either liquid or gas attack the strained silicate or oxide bonds at the crack tip causing them to increase in size. Slow crack growth occurs also at high temperatures because increased atom mobility and decreases in boundary phase viscosity can lead to intergranular crack growth.

In order to minimize the effect of SCG, glass samples that were vacuum packed were kept in their original packages until ready for ALD processing. All washed glass was dried immediately after washing. Heating-only tests were conducted prior to ALD coating tests to ensure that heating itself did not weaken the samples. The possibility that water as an ALD precursor contributed to SCG was also considered. For this reason some aluminum oxide coatings were grown using TMA and ozone as precursors. As a last precautionary measure, glass articles that were laminated were tested shortly after lamination because soap water was used in the manual attachment of the anti-splinter films on the glass surfaces.[24]

3.7 Weibull reliability analysis

Glass specimen strengths vary because of variations in the size, severity, location, and density of flaws. This variability in strengths is often analyzed using the Weibull distribution which presumes that the weakest link in a body controls strength. In other words, if a glass specimen has a large number of flaws with failure strengths that will be independent and identically distributed and the glass breaks because of the most severe flaw, the Weibull distribution can provide a good description of the system's failure-strength distribution. The Weibull distribution is frequently

used in reliability applications. The normal distribution is not used because the random variable representing the fracture strength assumes only positive values and the distribution is asymmetric about the mean. The continuous random variable x has a two-parameter Weibull distribution if the probability density function is given by [25]:

$$f(x) = \left(\frac{m}{\beta}\right)\left(\frac{x}{\beta}\right)^{m-1} \exp\left[-\left(\frac{x}{\beta}\right)^{m}\right] \quad x > 0 \tag{8}$$

$$f(x) = 0 \qquad x \leq 0 \tag{9}$$

The corresponding cumulative distribution function is given by [25]:

$$F(x) = 1 - \exp\left[-\left(\frac{x}{\beta}\right)^{m}\right] \quad x > 0 \tag{10}$$

$$F(x) = 0 \quad x \leq 0 \tag{11}$$

In equations (8) and (10) m is the Weibull modulus or shape parameter (>0) and β is the scale parameter (>0). The Weibull modulus is a measure of the width of the Weibull distribution (variability in measured material strength). The scale parameter is also called the characteristic strength, which is the strength value at a probability of failure of 0.632. For this reason it is often known also as the B63 value.

There are a number of ways to estimate the parameters of the underlying distribution, including ordinary least squares (OLS), moments, and maximum likelihood (ML) methods. ML and median-rank regression (MRR, which is based on OLS) methods are most commonly used today. In this work the parameters have been estimated using the ML method. According to the EN 843-5 standard [25] this estimator is the most efficient for small sample numbers based on producing a smaller coefficient of variation of the Weibull modulus. In addition, many statisticians advocate the use of ML because of its well-known distributional optimality properties in large samples. Results of an extensive simulation study by Genschel and Meeker [26] show a strong preference for the ML method for situations arising in practical reliability analysis. In their experience, for samples of moderate size (e.g. 20-30) it seemed impossible to find anything that will be consistently better than an ML estimator.

In contrast, OLS regression estimators are linear estimators that put large weight on the extreme observations having large variance. In probability plots (discussed later) an MRR estimate will go through the points even when it should not, giving highly misleading results.[27]

Often concurrent, compound or exclusive flaw distributions exist in a population. This can lead to a bimodal or multimodal distribution of strengths. Because in such cases the two-parameter Weibull distribution cannot validly be fitted to the

data, a graphical representation, namely a Weibull probability plot, is helpful for deciding whether a Weibull analysis can usefully be made. In case such an analysis is determined to be valid, the likelihood function (12) is utilized to find estimates for the Weibull modulus $\hat{m}$ and characteristic strength $\hat{\sigma_0}$ [25].

$$L = \prod_{j=1}^{N} \left(\frac{m}{\sigma_0}\right) \left(\frac{\sigma_{fj}}{\sigma_0}\right)^{m-1} \exp\left[-\left(\frac{\sigma_{fj}}{\sigma_0}\right)^{m}\right] \tag{12}$$

where N = number of fracture data

Function (12) is maximized by differentiating the log likelihood (ln(L)) with respect to m and σ_0, and setting the resulting functions equal to zero [25].

$$\frac{\sum_{j=1}^{N} \sigma_{fj}^{\hat{m}} \ln \sigma_{fj}}{\sum_{j=1}^{N} \sigma_{fj}^{\hat{m}}} - \frac{1}{N} \sum_{j=1}^{N} \ln \sigma_{fj} - \frac{1}{\hat{m}} = 0 \tag{13}$$

and

$$\hat{\sigma_0} = \left[\left(\sum_{j=1}^{N} \sigma_{fj}^{\hat{m}}\right) \frac{1}{N}\right]^{1/\hat{m}} \tag{14}$$

Equation (13) is solved numerically to obtain a solution for $\hat{m}$, which is then used to solve for $\hat{\sigma_0}$ using equation (14). Standard EN 843-5 recommends a fractional accuracy of solution (ϵ) to be ≤ 0.001, giving three significant digits in the value of $\hat{m}$. This estimate for the Weibull shape should be bias-corrected (refer to the standard for details). For the ML method, the magnitude of the bias decreases with increasing sample size. There is minimal bias in the characteristic strength estimator and thus it does not need to be adjusted.

In this study no data was censored because separation of the test data into subpopulations by flaw type is not recommended without clear fractographic confirmation that the separation is justified.

The Weibull probability plot introduced above is constructed by ranking the strength data from weakest to strongest and plotting it on a special set of axes that linearize the data. Data that fits the Weibull distribution fits also on a line with a slope equal to the Weibull modulus. Weibull plots presented in the results section have been produced using the Minitab 16 statistical software. The abscissas of the Weibull probability plots represent the failure stresses of each broken glass specimen, except in case of the BOR tests where failure forces (N) were not converted into stresses (MPa). The failure stress is calculated from the recorded failure force using equation (15). In this equation, F is the failure force recorded by the materials testing machine at the time of failure; L is the separation between the supporting edges, l the separation between the loading edges, b and h the width and thickness of the specimen, respectively. The ordinates are calculated using the modified Kaplan-Meier (Hazen) routine [29]. Each data point is assigned a probability value in

accordance with the ranking estimator (equation (16)).

$$\sigma = \frac{3F(L-l)}{2bh^2} \tag{15}$$

$$P_{fi} = \left(\frac{i-0.5}{N}\right) \tag{16}$$

for the i^{th} ranked data point of strength σ_{fi}.

4 Results

4.1 General observations

4.1.1 Thin film layer thickness accuracy and precision

There were altogether 77 aluminum oxide ALD processes completed with a P400 ALD system during the course of the study. The average absolute deviation from the target for these processes was -0.31nm (see Figure 20). The average percentage deviation from the average measured thickness (see equation (7)) was 1.48%. This means that for a coating that was on average 50nm thick, the thickness stayed within 1nm of this average. See Figure 21 for details.

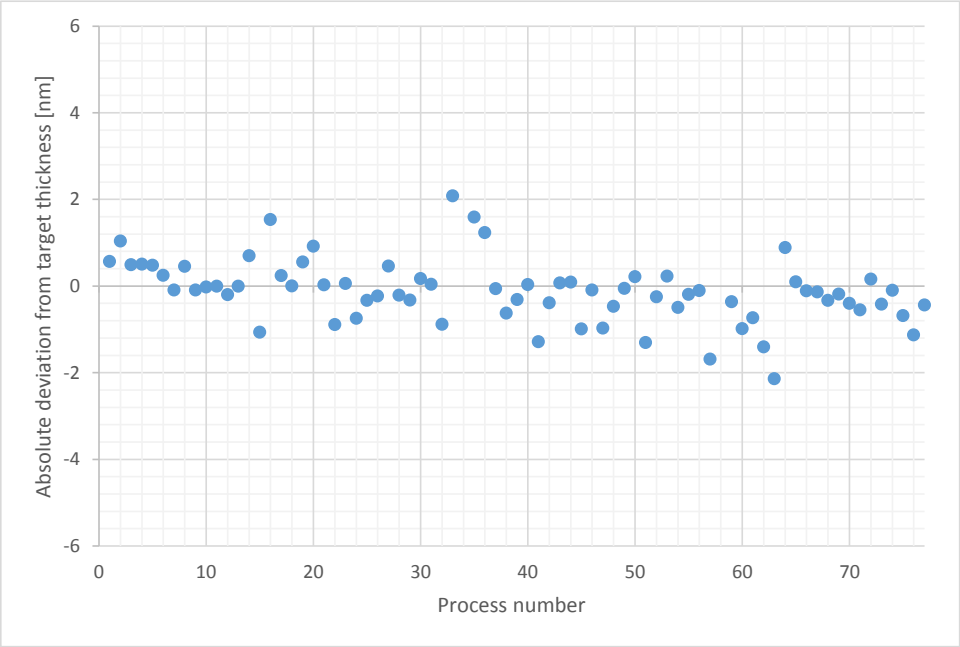

Figure 20: Absolute deviation of actual measured thickness from target thickness of all 77 Al_2O_3 P400A ALD system processes in nanometers.

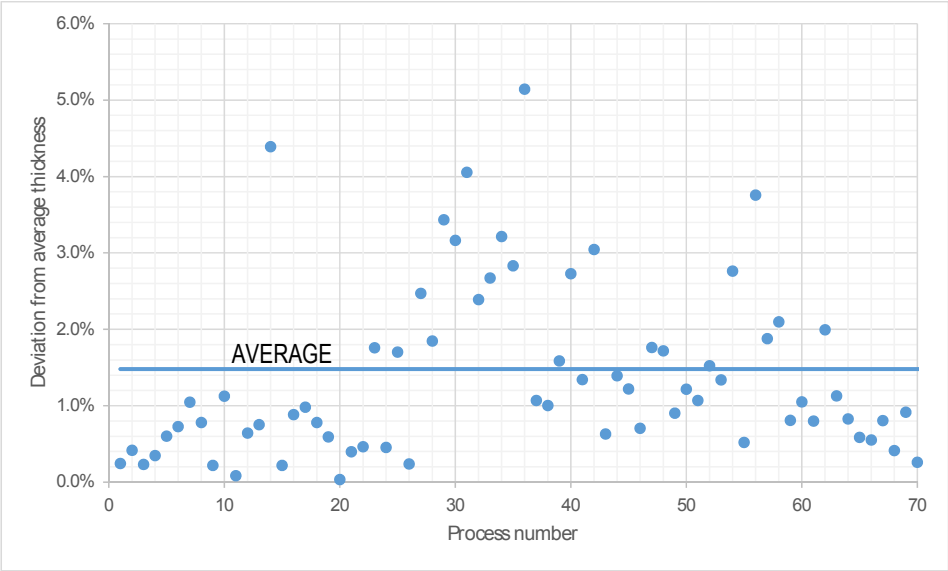

Figure 21: Thickness uniformity of 77 Al_2O_3 P400A ALD system processes.

4.1.2 GPC as a function of temperature

All ALD processes were monitored in terms of layer thickness with small pieces of silicon (see Figure 13) placed at various locations inside the ALD reaction chamber. Figure 22 shows the relationship between ALD reaction chamber temperature and growth as Ångstroms per cycle. At first GPC increases with temperature but this relationship reverses at higher temperatures. Peak GPC is reached at around 200°C.

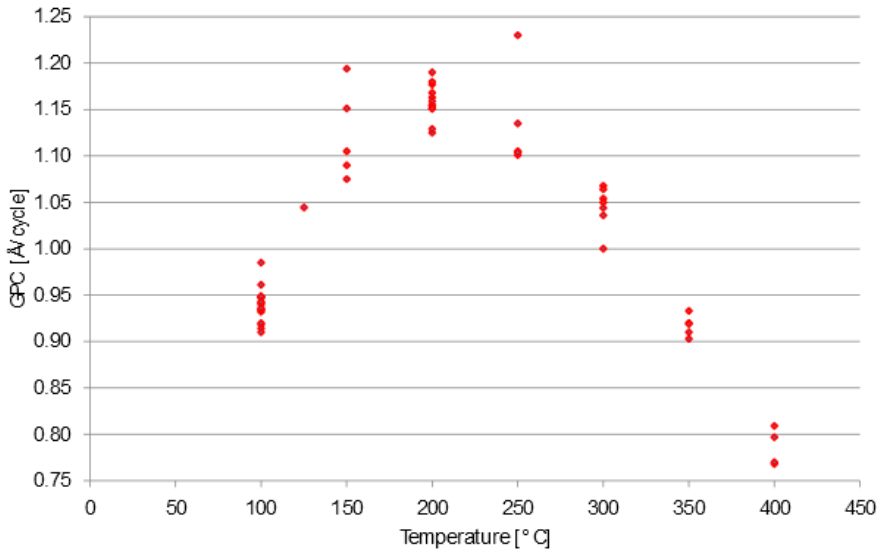

Figure 22: Growth-per-cycle (GPC) as a function of temperature. The pulse and purge times were changed according to process temperature.

4.1.3 Repeatability of the ALD process and mechanical testing

In some of the experiments, bending test results of two sets with identical ALD processing were compared in order to observe ALD process and mechanical testing repeatability (See Figure 23 and Figure 24). In all of the Weibull plots the line number of the variable box corresponds with the same line number in the table of statistics box. For example, the shape and scale of Process A set are 6.38482 and 68.218 respectively. The higher the shape, the lower the variability of strengths within a set, and the steeper the slope of the line running through the data points of a set. The AD* seen in the table of statistics box is the Anderson-Darling statistic. It measures how well the data follow a particular distribution, in this case the Weibull distribution [32]. F stands for number of failures, or number of samples within a set, and C corresponds to the number of samples that were censored (always zero because no censoring was done in this study).

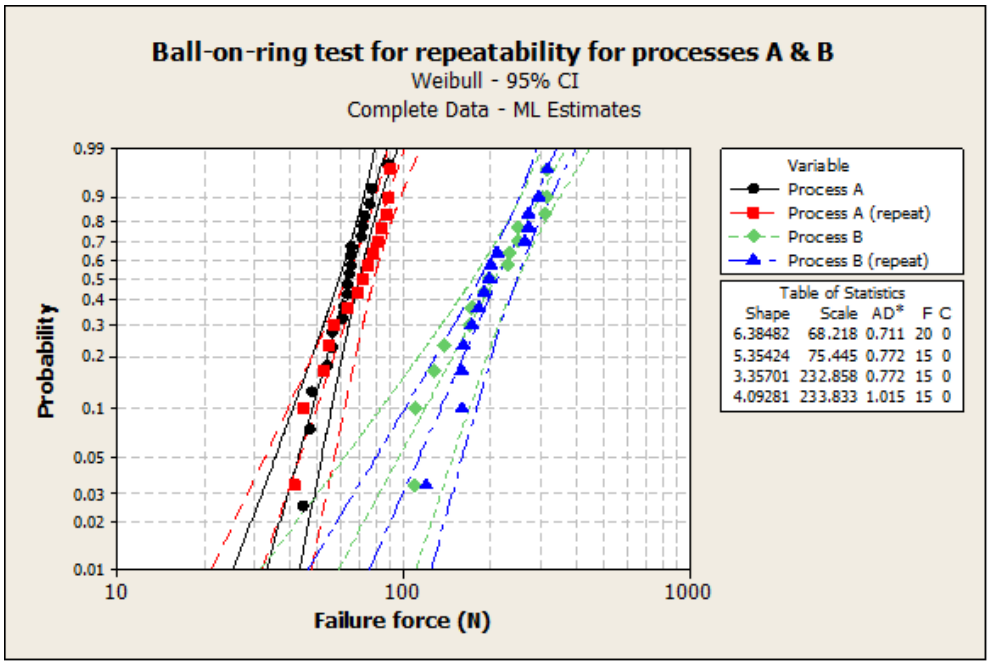

Figure 23: Ball-on-ring test reveals good repeatability for processes A and B (non-IOX glass).

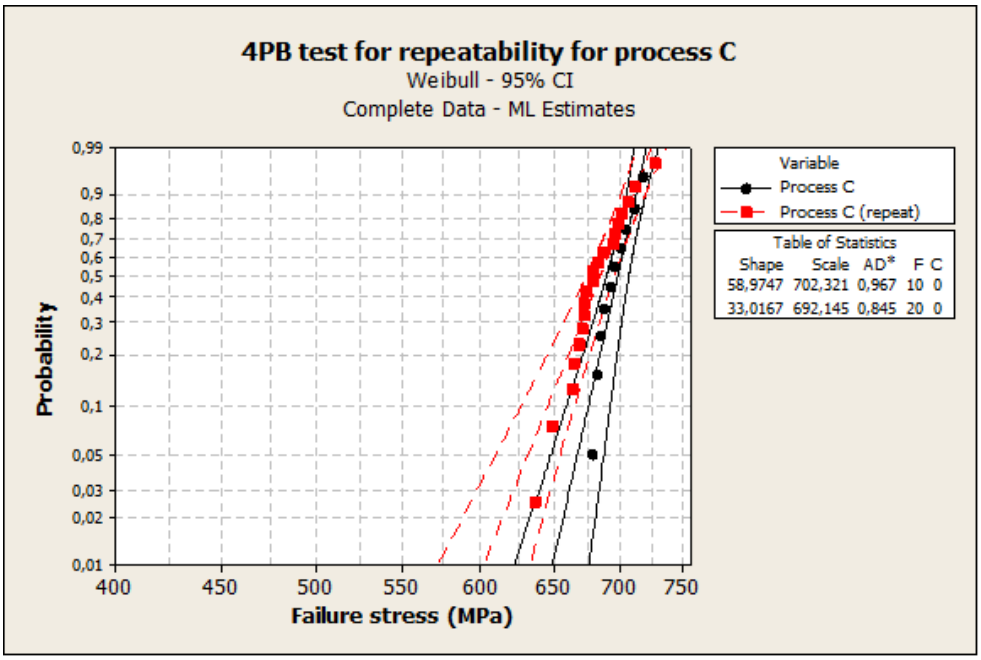

Figure 24: 4PB test shows good repeatability for process C (IOX glass).

4.1.4 Effect of lamination

Lamination of glass with an anti-splinter film before testing did not seem to have an effect on the bending strength. For non-prestressed glass a 2-sample t-test gives a P-value of 0.615, and for chemically strengthened glass a P-value of 0.59. Although the 2-sample t-test assumes population normality, yet it is often valid even when samples come from non-normal populations like the Weibull distribution.

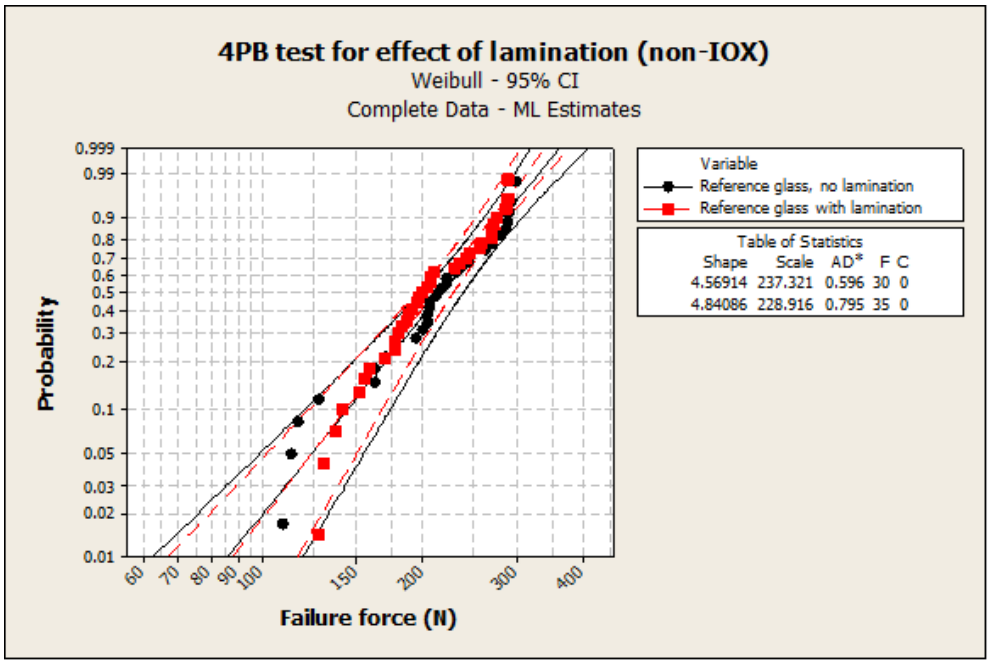

Figure 25: 4PB test for effect of lamination on bending strength for non-IOX reference glass (no ALD coating).

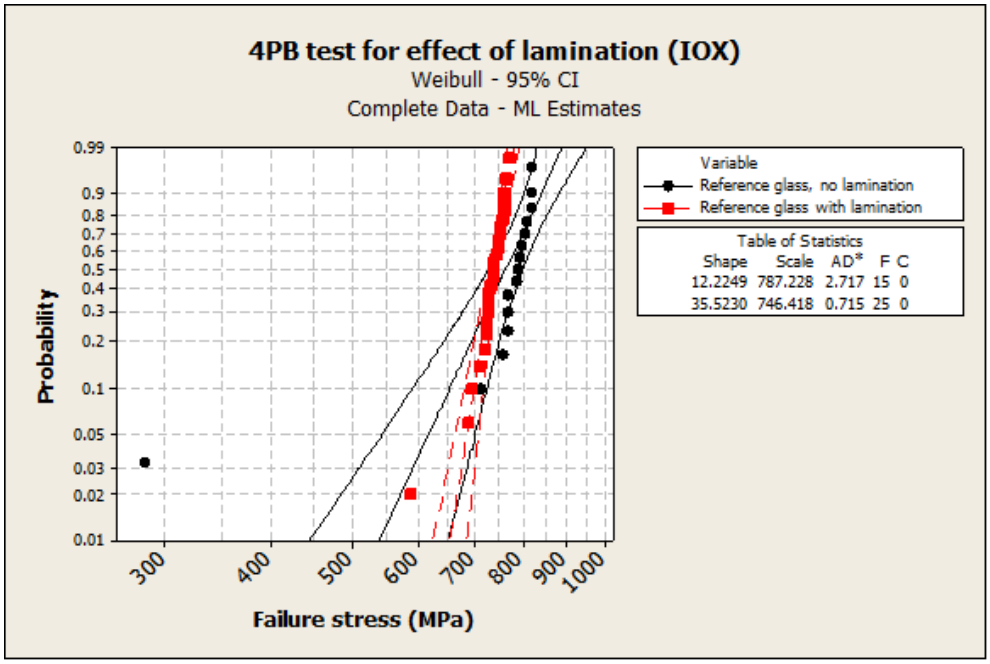

Figure 26: 4PB test for effect of lamination on bending strength for IOX reference glass (no ALD coating). Even if the outlier of the set without lamination is included, the 2-value t-test confirms that there is no significant difference between the two sets.

4.1.5 Optical transmission

A study of transmission for different ALD process conditions was conducted for one type of chemically strengthened glass with a double-sided coating. As can be seen in Figure 27, transmission decreases on average in the visible range by 1% for a 15nm coating, and by 3-4% for a 40nm coating.

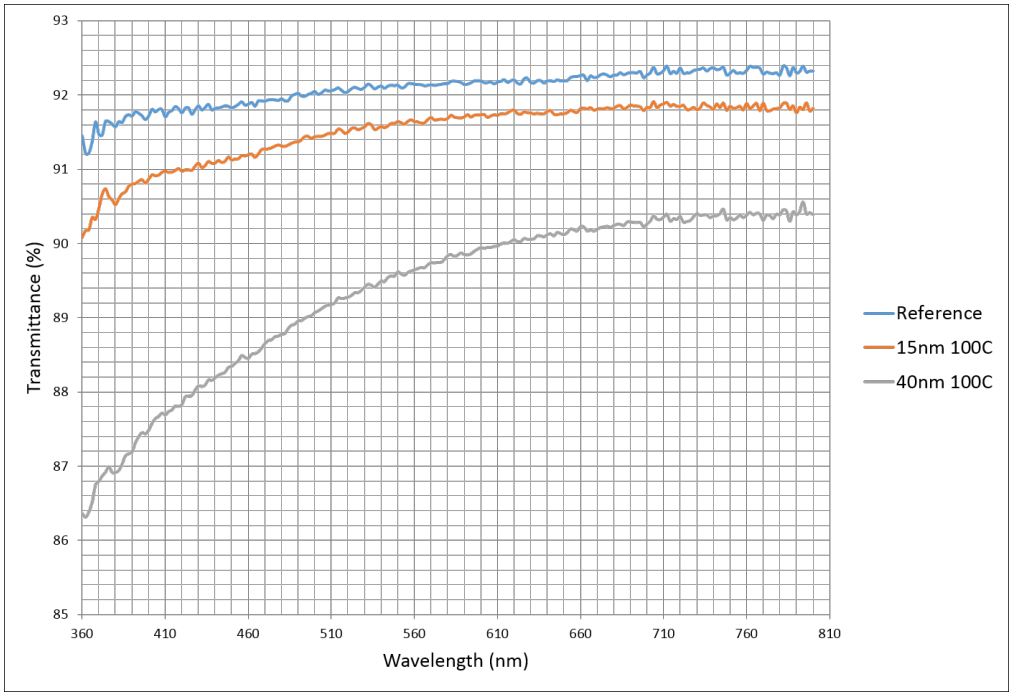

Figure 27: Optical transmission of chemically strengthened glass with two different double-sided ALD coatings. Note that the indicated thicknesses refer to layer thickness per side. The total layer thickness is 30nm (twice the 15nm on both sides of the glass) and 80nm.

4.2 Chemically strengthened glass experiments

4.2.1 Effect of heating

As mentioned previously, the effect of heating without coating was studied for several types of chemically strengthened glass. Heating tests were conducted as a rule at the beginning of each new set of tests for a new type of glass. Figure 28 shows how the characteristic strength of the reference sets is almost always higher than that of those sets that were heated for several hours. There is also a nearly inversely proportional relationship between temperatures and the characteristic strength: the higher the temperature, the lower the strength. At 200°C the strength cannot be said to drop significantly, if at all. The same can be said about 250°C. Changes start to occur around 300°C. Within the 300-350°C range, the characteristic strength drops roughly 10-15%.

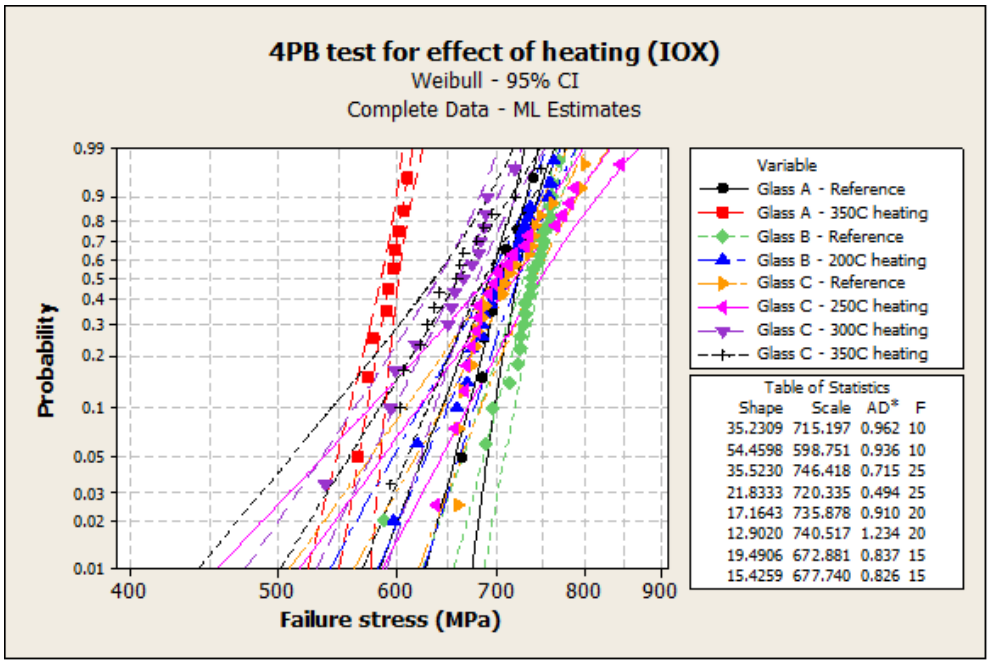

Figure 28: 4PB test for effect of heating on bending strength for IOX glass (no ALD coating). Note the considerably higher shapes for IOX glass as compared with non-IOX glass in Figure 31.

4.2.2 4PB flexural strength tests for coated samples

Improvement in the flexural strength of chemically strengthened glass was very challenging and gave contradictory results. Figure 29 shows one of the best results with glass type A: improvement in B63 as compared to reference glass was approximately 12%, and as much as 22% in B10. However, a repeat of this did not yield as great of an improvement. As the ALD and mechanical testing processes were determined to be robust and highly repeatable, the reason for the drop in strength down to about 6% (see Figure 30, glass type A) could be due to the fact that the glass used in the repetition test did not come from the same batch as the original set.

Figure 30 shows the percentage improvement in the characteristic strength (B63) of the best set with certain ALD process conditions as compared to a reference set from each glass type. Best improvements stay below 20%. This is understandable as chemically strengthened glass is by itself already very strong. Even the slightest changes in the way glass has been pre-processed or handled can significantly affect the results.

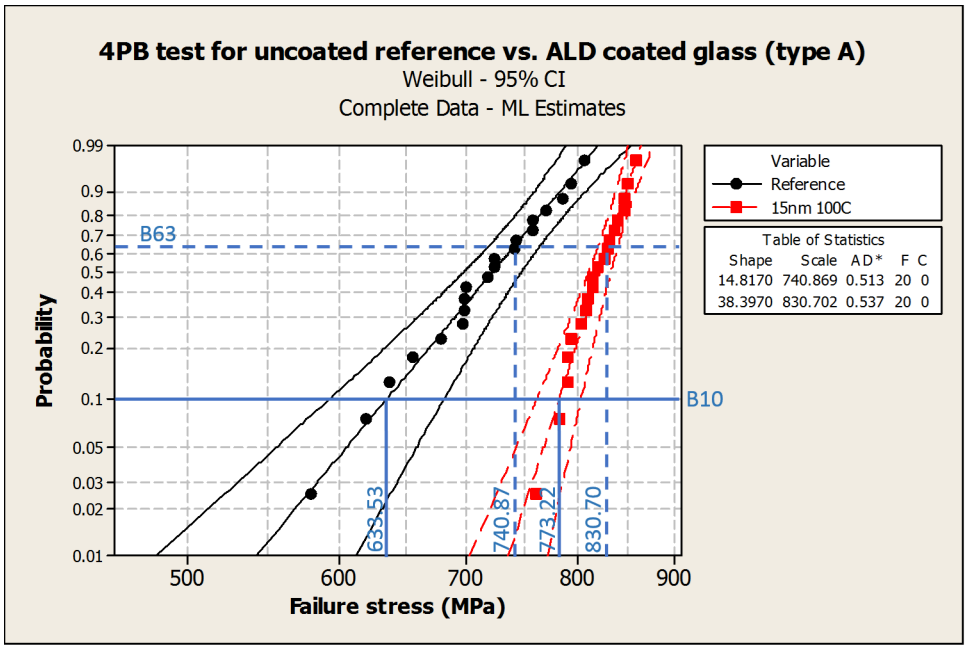

Figure 29: 4PB test result for chemically strengthened, uncoated reference glass versus chemically strengthened, ALD coated glass. Improvement in B63 is about 12 percent, and 22 percent for B10. The B63 value is the characteristic strength, which is the strength value at a probability of failure of 0.632.

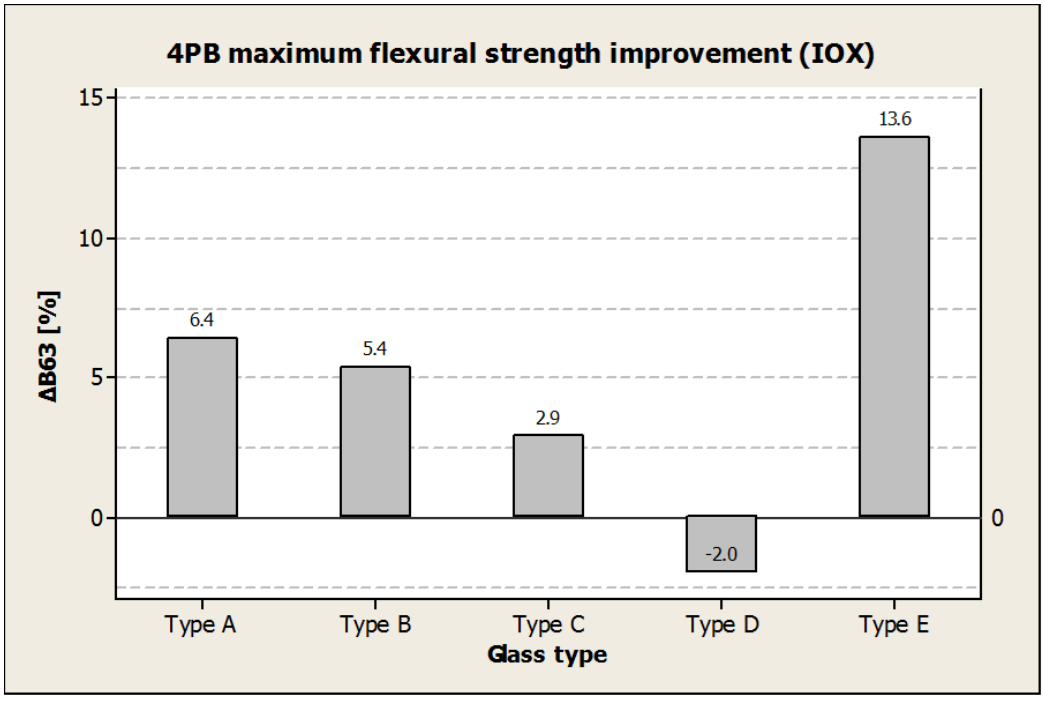

Figure 30: 4PB test results for five different chemically strengthened glass types. ΔB63 shows the percentage improvement in B63 of ALD coated glass as compared to uncoated reference glass.

4.3 LCD glass experiments

Aluminosilicate LCD glass was tested extensively with over 60 test sets and 1600 test specimens. The effects of mechanical washing, lamination and failure modes, side under tension and scribing side were studied in detail. The thickness of the LCD glass was 0.7mm.

4.3.1 Effect of heating

Heating-only experiments with aluminosilicate LCD glass lead to the conclusion that even temperatures as low as 200°C have a degrading effect on the flexural strength. B63 (scale) drops approximately -30% at 200-250°C, and over -35% at 300°C (see Figure 31 for a Weibull plot).

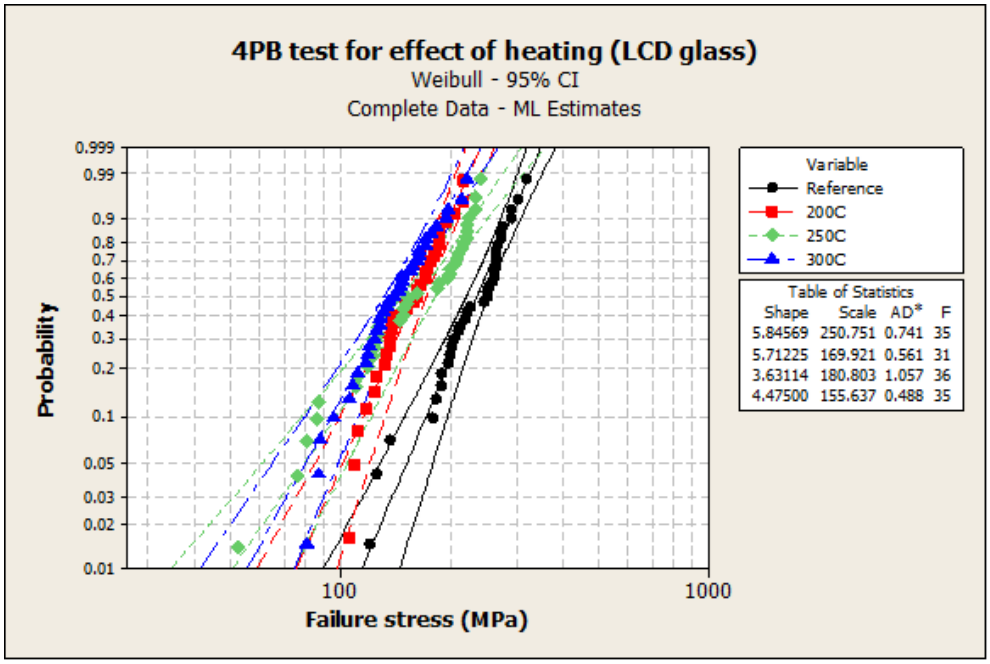

Figure 31: 4PB test for effect of heating on bending strength for aluminosilicate LCD glass (no ALD coating).

4.3.2 4PB flexural strength tests for coated samples

In order to ensure correct alignment of the jigs attached to the materials testing machine, the origin of fracture (edge or face) was recorded for each failed glass specimen. Almost 85% of fractures originated from the edges. The figure seems sensible because the four-point bending test is said to specifically test the edge strength. In addition, the origin of the edge cracks was distributed nearly symmetrically between the two long edges (approximately 60%/40%), indicating good jig alignment. The effect of washing was studied for most sets for both 4PB and BOR tests. Table

1 shows the 2-sample t-test P-values between washed and unwashed but otherwise similarly handled and ALD processed sets. 4PB results support the null hypothesis of there being no significant difference at the 0.05 significance level. BOR test results are somewhat similar with some exceptions (Set B and Set D).

Table 1: 2-sample t-test P-values between washed and unwashed but otherwise similar sets in both 4PB and BOR tests.

Set	4PB	BOR
A	0.074	0.195
B	0.417	0.000
C	0.717	0.749
D	0.421	0.000
E	0.047	0.593
F	0.281	0.053
G	N/A	0.292

A challenge lies with the reference sets used. For an unknown reason the washed reference set seems to be stronger than unwashed ones, even though intuition would indicate the contrary because of slow crack growth discussed in 3.6.1. Figures 32 and 35 indicate the noticeable gap between washed and unwashed reference sets.

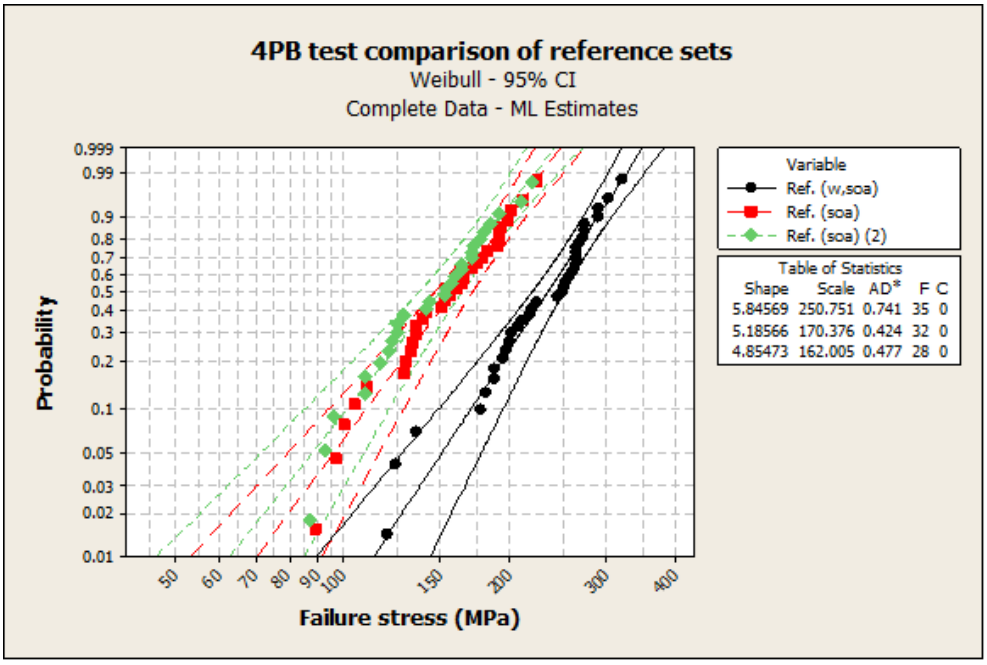

Figure 32: 4PB test comparison of one washed reference set and two unwashed reference sets. 'w' = washed, 'soa' = scribing on air side of the float glass.

As can be seen in Figure 32, two reference sets were tested for unwashed glass. Because the results of these two tests were in harmony with each other, they were compared to unwashed, coated sets. Figure 33 shows how all ALD coated sets were stronger than the reference sets (B63) by up to 65% (15nm at 200°C). The results are even better when the edges of glass samples were coated as well (see Figure 34). Edge coated sets showed improvements up to 76% (50nm 300C).

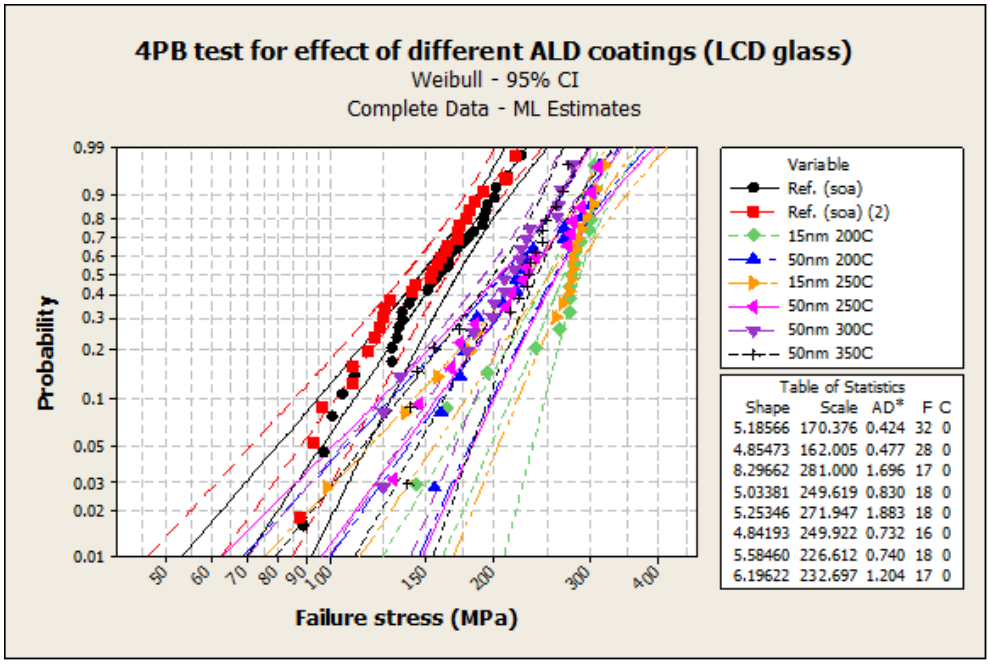

Figure 33: Weibull plot of 4PB tests for unwashed reference glass versus unwashed glass with different ALD coatings.

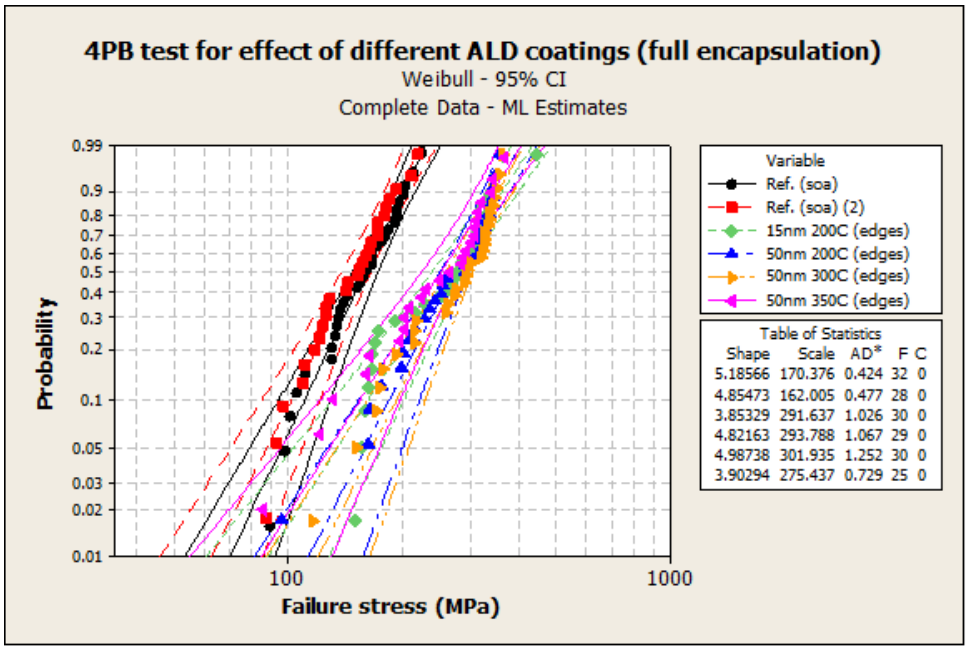

Figure 34: Weibull plot of 4PB tests for unwashed reference glass versus unwashed glass with different ALD coatings (also on edges).

4.3.3 BOR flexural strength tests for coated samples

Similarly to 4PB tests, washed and unwashed reference sets cannot be said to be equivalent (see Figure 35). A large standard deviation (even greater than in 4PB tests) in BOR tests is also evident. This is likely due to the small stress area of a BOR setup. Table 2 shows how BOR tests have on average a higher standard deviation (lower Weibull shape value) than 4PB tests.

Table 2: Average of shapes of BOR tests compared with that of respective 4PB tests.

Glass type	Average % change in Weibull shape
Glass A, non-IOX	-37%
Glass B, IOX	-62%

The strengthening effect is difficult to quantify for the BOR tests because of the large variation in the strength of the reference sets. For washed samples there is no more than 5% improvement in B63. However, regardless of the reference set used for unwashed samples, there is a 37-113% maximum strength improvement in B63 with 15nm coatings. Improvement with 50nm coatings is up to 40%.

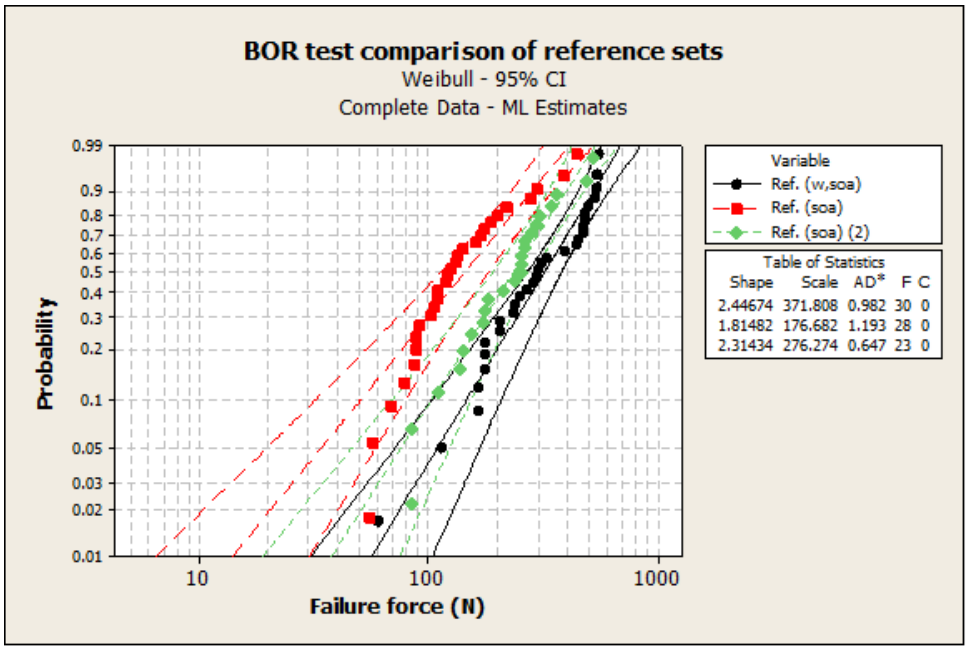

Figure 35: BOR test comparison of one washed reference set and two unwashed reference sets. Weibull scale ranges from 177 MPa to 372 MPa (or for two unwashed sets from 177 MPa to 276 MPa) which adds difficulty to comparison of test sets.

4.4 Ultrathin glass experiments

4.4.1 Effect of heating

Figure 36 shows a boxplot of BOR tests conducted to find out the effect of heating on glass samples of three different thicknesses, 100µm, 300µm, and 500µm. At this point it should be noted that the existing, standardized methods of flexural strength testing might not be valid for ultrathin glass.

There is no significant difference in strengths between reference and the 100°C sets for any thickness. In contrast, and as with chemically strengthened glass, 300°C temperatures seem to already have a noticeable effect. The B63 values drop so that the effect is for an unknown reason more pronounced for thicker glass. Table 3 shows the percentage changes in B63 as well as the 2-sample t-test P-values between reference, 100°C heating-only, and 300°C heating-only sets for the three glass thicknesses. At a 0.05 significance level the null hypothesis is accepted for all combinations. Thus, this test suggests that heating the glass for several hours does not weaken it significantly. Whatever the truth, temperatures above 300°C were used nonetheless because a positive strengthening effect of an ALD coating was believed to more than counterbalance any miniscule negative effect a higher process temperature might have. Moreover, should optimal conditions be found at higher temperatures where ALD films grow typically more conformably, the process might afterwards be tweaked in such a way as to minimize any negative side effects, for example, by shortening the pre-heating time.

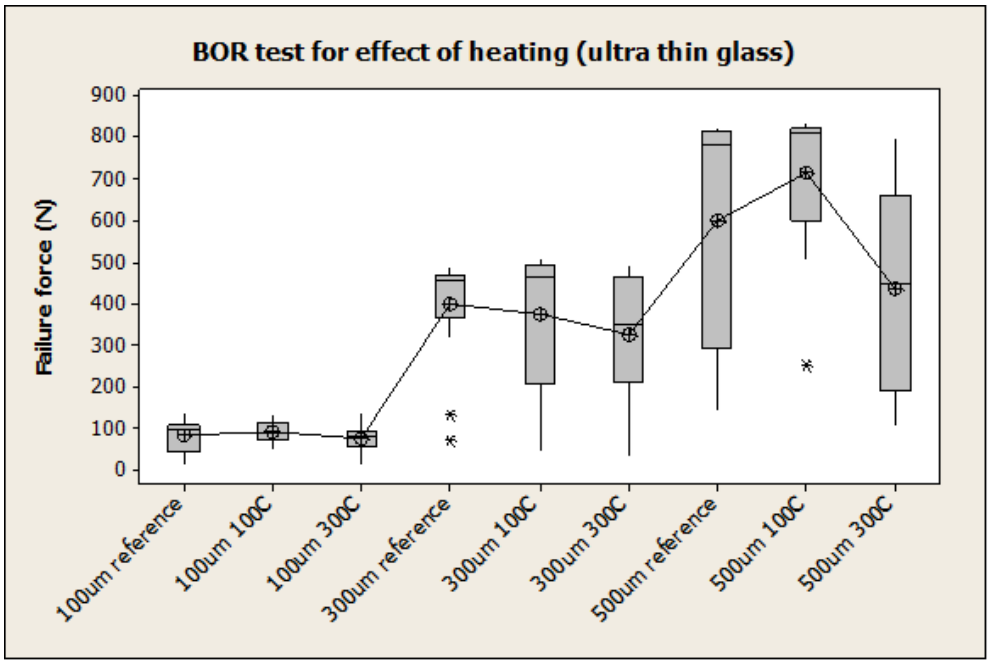

Figure 36: BOR test for effect of heating on bending strength for ultra thin glass (no ALD coating). Three different thicknesses of the same type of glass were heated at two different temperatures, 100°C (7.5 hours) and 300°C (5.5 hours).

Table 3: 2-sample t-test P-values and drop in B63 (characteristic strength) between reference, 100°C heating-only, and 300°C heating-only sets for three glass thicknesses. For example, the P-value for the reference versus 100°C heating-only sets (both 100µm thick) equals 0.426. At the 0.05 significance level the null hypothesis is accepted, meaning that the two sets can be said to be similar. The characteristic strength (B63) of the 100°C set is 8 percent stronger than that of the reference set.

	Reference		
	100µm	300µm	500µm
100°C	0.426 / +8.0%	0.625 / -4.0%	0.166 / +14.7%
300°C	0.723 / -5.5%	0.146 / -16.3%	0.082 / -27.0%

4.4.2 BOR flexural strength tests for coated samples

Only the BOR test setup was used for testing the ultra-thin glass. Similar tests were conducted for three different glass thicknesses: 500µm, 300µm, and 100µm. The 500µm thick glass was useful for reference even if it is not considered ultra-thin glass per se.

Preliminary tests were carried out for determining whether original size rectangular specimens could be cut in half in order to double the number of samples. The results showed that the cut pieces (squares) were clearly weaker than the original uncut, rectangular pieces though in theory edge quality should not affect BOR test-

ing. This effect was more pronounced with thinner glass. For this reason, it was determined that the shape of the test specimen was the reason for the difference in strength, and that all tests should be performed on the original, rectangular shaped specimens.

The results of the ultra-thin glass tests are the most interesting in this work despite the fact that no ALD coating improved the flexural strength (in fact, the opposite was true: all thin film coatings regardless of thickness weakened the glass). This is because there is a clear trend with all glass thicknesses. Evidently thicker coatings result in weaker glass. Also, the process temperature is directly proportional to strength, i.e. the lower the temperature, the weaker the glass becomes. See Figures 37, 38 and 39 for the Weibull probability plots.

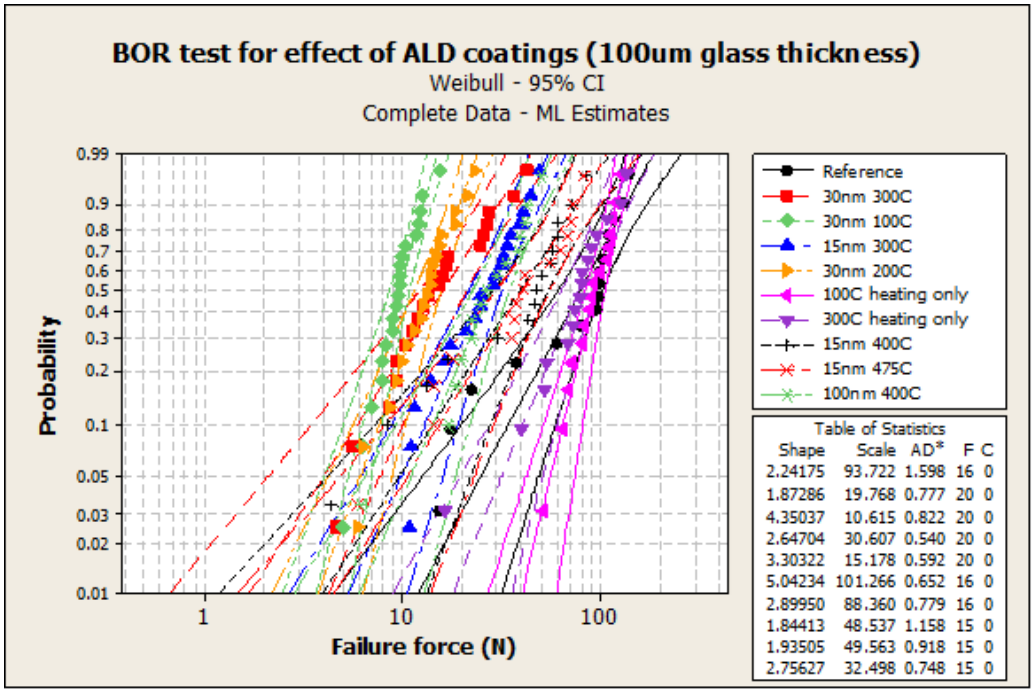

Figure 37: BOR test for effect of ALD coating on bending strength for ultra thin 100µm thick glass.

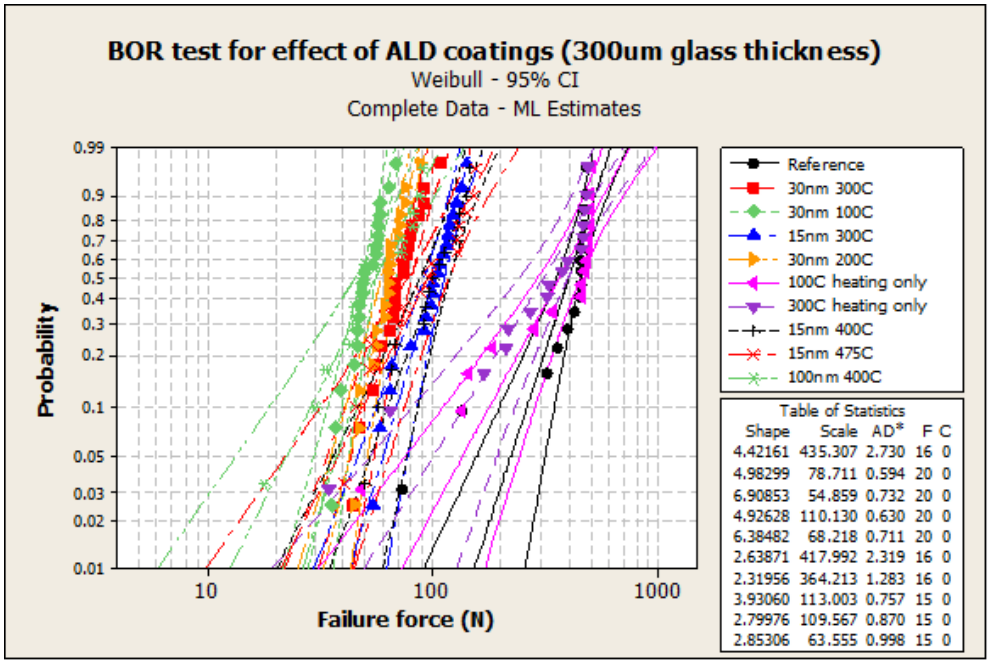

Figure 38: BOR test for effect of ALD coating on bending strength for ultra thin 300µm thick glass.

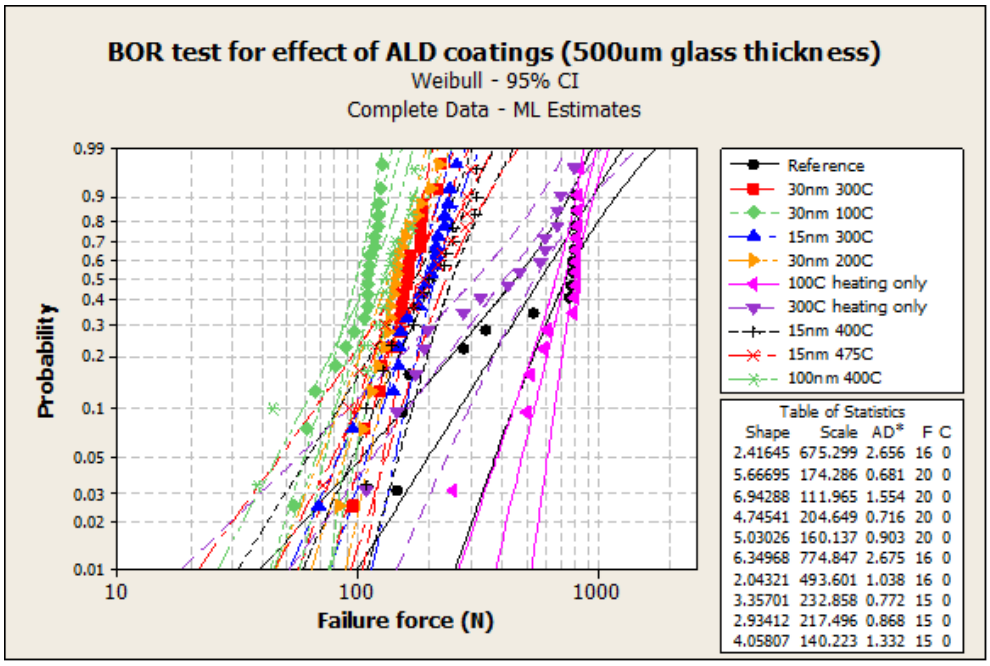

Figure 39: BOR test for effect of ALD coating on bending strength for 500µm thick glass.

As raising the process temperature while using thinner ALD layers did not result in stronger glass, titanium dioxide and a proprietary nanolaminate was used to investigate whether the observed weakening effect was due to stresses caused by a difference in the coefficients of thermal expansion (CTE) between the glass and the thin film. Figure 40 shows that while the choice of material does matter, none of the new materials helped to strengthen glass above its reference strength for the 300µm thickness. The effect was similar for the other two glass thicknesses.

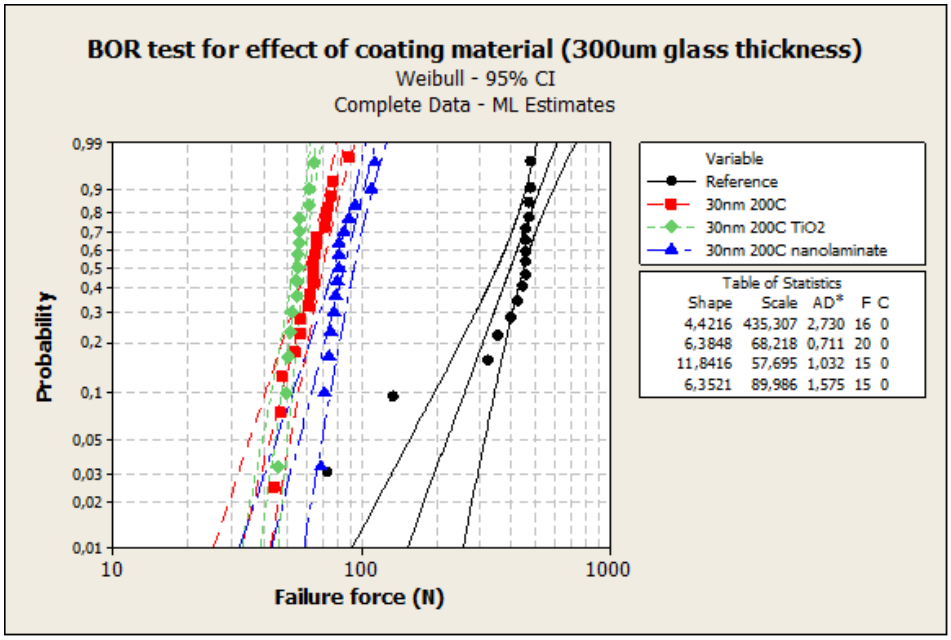

Figure 40: BOR test for effect of coating material on bending strength for 300µm thick glass.

In order to further confirm that the thin films really were the cause for weakening, new samples were coated on only one side. Consequently one set was tested with the thin film under tension, and another with the thin film under compression. The hypothesis was that if the side with the thin film was under compression, then the side under tension would be uncoated and the samples would be as strong as the reference. On the other hand, if the side with the thin film was under tension, then the strength should be similar to a fully encapsulated sample. This indeed was the case (see Figure 41). This single sided coating test confirmed that it is the coating that affects the flexural strength by a yet unknown reason.

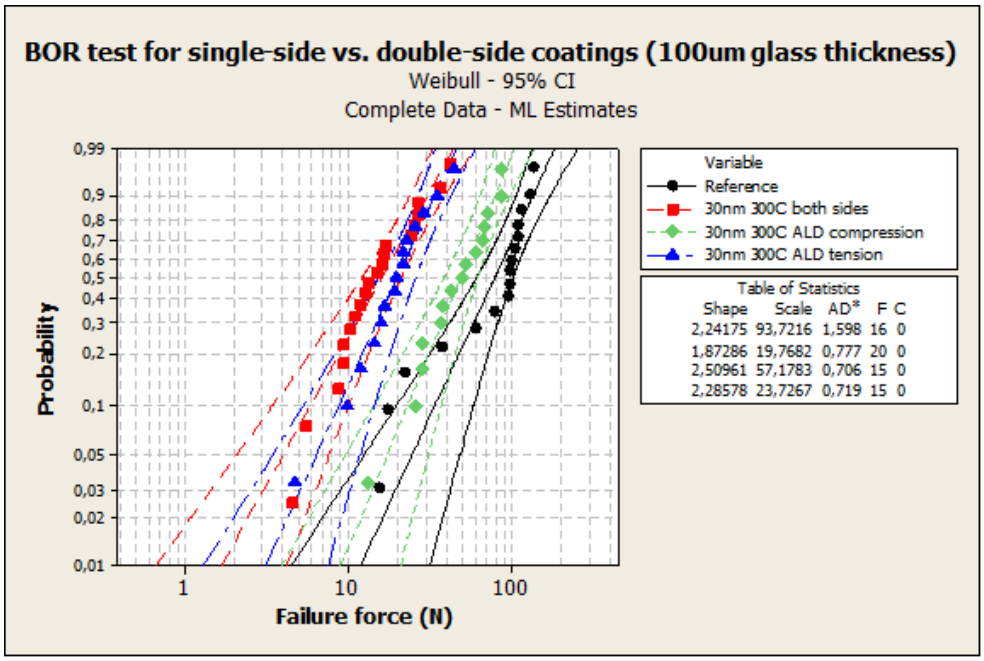

Figure 41: BOR test for effect of single side coating on bending strength for 100µm thick glass.

The last step in this study was to see whether friction between the testing machine jigs and the glass specimens affected the results. It was suspected that greater amounts of friction between the supporting ring and the glass would make it harder to flex the glass article because the loading ball would have to work against both the force resisting bending and the force resisting horizontal tension. In order to reduce friction, a PTFE foil was placed between the top side of the glass and the ball, and also between the bottom side of the glass and the ring (Figure 42). Using a PTFE foil did have an effect on the results but there was no clear trend evident. As stated above, the explanation as to the observed weakening is still to be discovered. However, one possible reason could be the use of water as one of the precursors in all the different processes used. In future experiments water could be replaced with ozone for the Al_2O_3process.

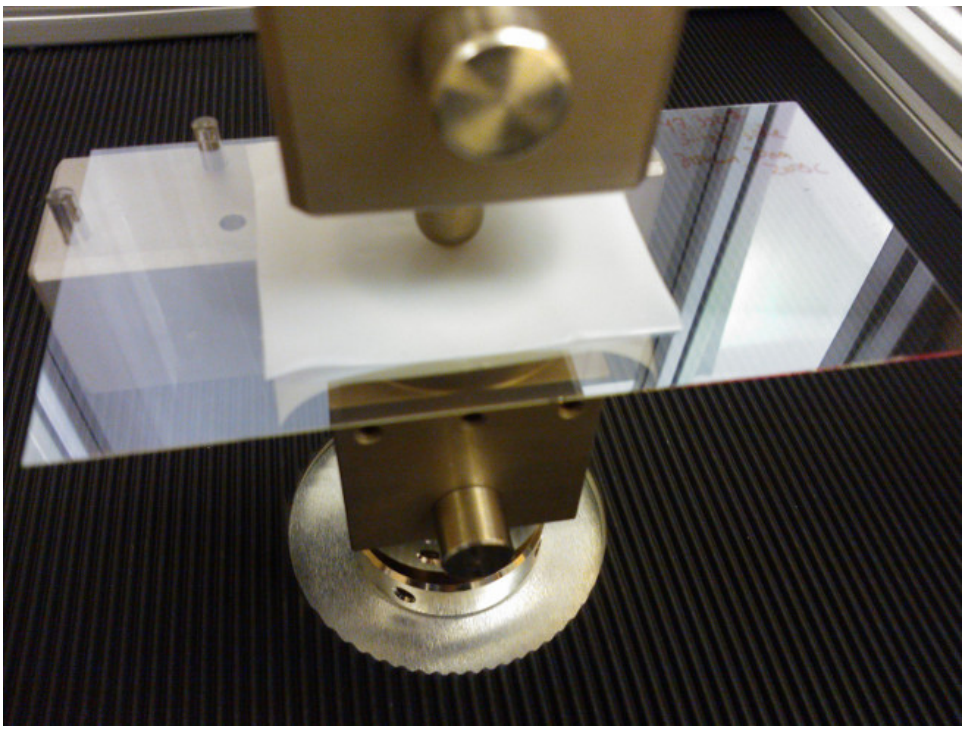

Figure 42: PTFE foils were placed under and on top of the glass specimen to reduce friction.

5 Conclusions

The primary objective of this thesis work was to develop an understanding of the best practices for preparing both non-strengthened and chemically strengthened glass for flexural strength tests, for testing the properly prepared glass, and to analyze the results using well known methods used for reliability analysis. This objective was met with valuable input from prominent glass manufacturers, reliability analysis laboratories and equipment distributors, and customers of glass products worldwide. The list below states the most important conclusions relating to the first objective.

1) The scatter in the results of LCD glass is probably at least partly due to the quality of scribing when performed at Beneq. Cutting of glass is best done by glass manufacturers specialized in the task to ensure homogeneous edge quality.

2) Glass to be coated should be ultraclean. Vacuum packing is favored.

3) Although the ALD process is highly repeatable, variations in the quality of glass could be misleading. Multiple batches with similar ALD process specifications is crucial in establishing clear indications of improvement. Even reference sets fluctuate so much that in order to establish a case one needs to get clear improvements (at least 10% in B63).

4) The 4-point bending test is preferred over the 3-point bending test (as also recommended in the aforementioned standard), and also over the BOR test. This is to maximize the area under stress. If the face strength is to be tested, then the equibiaxial flexural strength test (ring-on-ring) is preferred over the ball-on-ring test for the same reason.

5) Because cooling processes are usually much more critical than the continuous rapid heating of glass [8], more attention should be given to cooling after an ALD process, especially if higher temperatures are used.

6) Washing seems to change the properties of the LCD glass used. Other means of washing should be considered.

The second objective was to investigate the feasibility of using ALD grown thin films for strengthening of glass. Process temperature and layer thickness were to be optimized in order to achieve the greatest possible increase in strength.

What can be said about the ALD process itself is that it is very reliable and repeatable as to the layer thickness and conformity even in large batches, both within a single batch, or between different batches. The ALD process is industrially scalable, and there is clear evidence that ALD can be used for glass strengthening judging by previous research and the results of this work. How much improvement is possible is clearly dependent on the glass type and its pre-ALD treatment. Also, achieving clear and absolutely reliable improvements requires careful preparation because the whole process including pre-treatment by glass manufacturers is rather complex.

In some cases bare glass without chemical strengthening has increased in strength by over 100%. In contrast, further strengthening of chemically strengthened glass is more challenging. In this work, the best results were around 20%. This is logical because chemically strengthened glass by itself is already very strong. It appears that in this case even small deviations in the pretreatment of this glass type can have a dramatic effect on the result. In effect, the original aim to replace time-consuming and more expensive processes related to chemical strengthening is to be postponed for the time being.

For LCD glass the results were promising, but more tests should be completed to establish clear trends.

The ultra-thin glass experiments were the most interesting despite the drop in strength. It was evident that heating by itself did not weaken the glass, but even a thin 15nm layer caused a near 70% loss of the original B63 strength. Interestingly the drop for a 30nm thick layer was even greater, close to 90%. The use of ultra-thin glass revealed perhaps the most important discovery in this study: that a layer as thin as a few dozen nanometers can cause such a dramatic effect on the strength of glass.

The most crucial question then is, what is the mechanism that causes it? Is the observed weakening occurring because of a thin layer exerting coefficient of thermal expansion related stress on the cracks or because of another reason? Research into this phenomenon could provide answers to not only effects caused on ultra-thin glass but also on other glass types (the effect could be the same with stronger glass, but less evident). In effect, should the cause be related to difference in thermal expansion of glass versus a thin film, perhaps a new material or method of producing a thin film could lead into an opposite effect.

As a conclusion, based on the findings of this work the following topics are suggested for further research:

1) Acquisition of more data on the effect of thin films on ultra-thin glass

2) Application of considerably thicker aluminum oxide thin films even at the expense of lost transparency. Later, the material could be changed to a more transparent one such as silicon dioxide.

3) Effect of cooling time on strength

4) Using smaller batch sizes for coating. This way one test cycle will take less time due to a shorter heating time (alternatively, the specimen size can be decreased). Especially with ion exchanged glass smaller sample count per test set is acceptable because of lower variance, and, in any case increases in strength must most certainly be significantly greater than 10%.

Finally, in addition to the above list, over the course of the practical work of this study, collaboration with glass manufacturers and other entities within the field of business has attracted more interest in other uses of thin films such as scratch resistance. These can also be further explored in the near future to enhance the attractiveness of glass in modern applications.

References

[1] Abrisa Technologies, *Glass Strengthening Technical Reference Document*, November, 2012. Availability: http://www.abrisatechnologies.com/specs/

[2] Abrisa Technologies, *Guide to Glass Optical Properties*, March, 2012. Availability: http://www.abrisatechnologies.com

[3] Griffith, A. A., The Phenomena of Rupture and Flow in Solids, *Philosophical Transactions of the Royal Society of London. Series A, Containing Papers of a Mathematical or Physical Character*, 1921, vol. 221, 163-198.

[4] Grigoras, K., Franssila, S., Airaksinen, V.-M., Investigation of sub-nm ALD aluminum oxide films by plasma assisted etch-through, *Thin Solid Films*, 2008, vol. 516, 5551-5556., doi: 10.1016/j.tsf.2007.07.121.

[5] Asahi Glass Co., Ltd., Reference presentation, August 2012, Availability: www.agc.com/english/ir/library/gaiyou.html (accessed February 25, 2013)

[6] Suntola, T. and Antson, J. U.S. Patent No. 4,058,430 (15 Nov 1977)

[7] Puurunen, R. L., Surface chemistry of atomic layer deposition: A case study for the trimethylaluminum/water process, *Journal of Applied Physics,* vol. 97, 121301 (2005), doi: 10.1063/1.1940727

[8] Schott North America, Inc., Schott Technical Glasses - Physical and technical properties, Mainz, February 2010.

[9] 1911 Encyclopedia Britannica/Glass, *Wikisource, The Free Library*, Availability: http://en.wikisource.org/w/index.php?title=1911_Encyclop%C3%A6dia_Britannica/Glass&oldid=4201956 (accessed February 22, 2013)

[10] Encyclopædia Britannica Online, s. v. "industrial glass", accessed February 25, 2013, http://www.britannica.com/EBchecked/topic/234890/industrial-glass/76355/Tubes-and-rods.

[11] Pitbladdo, Richard B. (Horseheads, NY), U.S. Patent No. 6748765 (15 Jun 2004), http://www.freepatentsonline.com/6748765.html

[12] Pitbladdo, Richard B. (Naples, FL, US) Overflow downdraw glass forming method and apparatus, U.S. Patent No. 6990834 (01 Jan 2006), http://www.freepatentsonline.com/6990834.html

[13] Brunello, P. Fredholm, A. M. Gille, C. F. M. Madi K., Tellier, X. Fusion draw apparatus and methods, U.S. Patent No. WO/2012/158232 (22 Nov 2012), http://www.freepatentsonline.com/WO2012158232.html

[14] Huey-Jiuan Lin, Wei-Kuo Chang, Design of a sheet forming apparatus for overflow fusion process by numerical simulation, *Journal of Non-Crystalline Solids*, Volume 353, Issues 30-31, 1 October 2007, Pages 2817-2825, ISSN 0022-3093, 10.1016/j.jnoncrysol.2007.06.022, Availability: http://www.sciencedirect.com/science/article/pii/S0022309307006680

[15] Corning Inc., Availability: http://www.corning.com/displaytechnologies/en/about_us/process.aspx, accessed 26 Feb 2013.

[16] Gy, René, Ion exchange for glass strengthening, *Materials Science and Engineering B-advanced Functional Solid-state Materials*, Volume 149, Issue 2, 2008, Pages 159-165, doi: 10.1016/j.mseb.2007.11.029.

[17] Corning Inc. Technical Materials, Corning Gorilla Glass (Code 2318) - Chemical tempering procedures, Issued September 2007.

[18] Beneq Oy, Strengthened glass application brochure, Availability: www.beneq.com/strengthened-glass.html, accessed: 01 Sep 2012.

[19] Dittmar, G., Brunn S., Richter U., SE400 advanced operating manual, *Sentech Instruments GmbH*, 10.4.2007, version October 2007.

[20] Beneq Oy, P400A and P800 brochure, May 2010. Availability: www.beneq.com.

[21] Ametek, Inc./Lloyd Instruments Ltd., LR Plus User Manual, part no. 01/3083, ver. 3.0, February 2004. Availability: www.lloyd-instruments.co.uk.

[22] ASTM Standard C1499-05, 2005, Standard Test Method for Monotonic Equibiaxial Flexural Strength of Advanced Ceramics at Ambient Temperature, *ASTM International*, West Conshohocken, PA, 2005, DOI: 10.1520/C1499-05, www.astm.org.

[23] European Standard EN 1288-5:2000, 2000, Glass in building - Determination of the bending strength of glass - Coaxial double ring test on flat specimens with small test surface areas, British Standards, www.bsigroup.com.

[24] Quinn, George D., NIST Recommended Practice Guide - Fractography of Ceramics and Glasses, Special Publication 960-16, *National Institute of Standards and Technology*, 2007, Availability: bookstore.gpo.gov.

[25] European Standard EN 843-5:2006:E, Advanced technical ceramics - Mechanical properties of monolithic ceramics at room temperature - Part 5: Statistical analysis, *European Committee for Standardization*, ICS 81.060.30.

[26] Genschel, U., Meeker, William Q., A Comparison of Maximum Likelihood and Median Rank Regression for Weibull Estimation, *Department of Statistics, Iowa State University*, 2010.

[27] Minitab Knowledgebase/FAQ, Least squares (LSXY) estimates versus maximum likelihood estimates (MLE), ID 767, 2009.

[28] Abramov, Anatoli A., Black, Matthew L., Glaesemann, G. Scott, Laser separation of chemically strengthened glass, *Physics Procedia, Elsevier B.V.*, Vol. 5, Part B, 2010, Pages 285-290, doi: 10.1016/j.phpro.2010.08.054, ISSN: 1875-3892.

[29] Minitab guide, Graphing Data, Availability: http://cms3.minitab.co.kr/board/minitab_data/9.%20GraphingDataAllTopics.pdf

[30] Score Asia Technology Ltd., Kawaguchiko SS-451CP brochure, www.scoreasia.com.hk/machinery.html.

[31] ASTM Standard C158-02(2007), 2007, Standard Test Methods for Strength of Glass by Flexure (Determination of Modulus of Rupture), *ASTM International*, West Conshohocken, PA, 2007, DOI: 10.1520/C0158-02R07, www.astm.org.

[32] Minitab Inc., Minitab 16 StatGuide (found in the Help menu of the Minitab 16.2.3 software).

[33] Verterra, Romel T. F., Flexure Formula, MATHalino.com - Online Engineering Math Reviewer, 2009, Availability: www.mathalino.com.

[34] Wikipedia, List of moment of areas, 2013, Availability: http://en.wikipedia.org/w/index.php?title=List_of_moment_of_areas&oldid=554789357.

[35] eFunda Inc., Derivation of Four Point Bend Test, 2006, Availability: www.efunda.com.

A Derivation of the 4-point and 3-point bending formulae

Consider the loaded beam in Figure A1.[33]

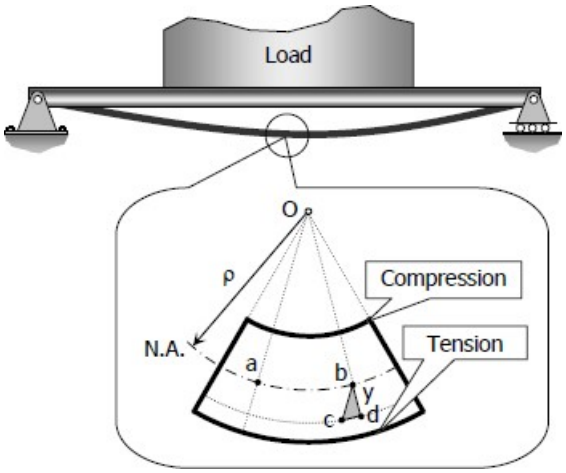

Figure A1: A beam is bent by applying a downward load. The upper surface of the beam falls under compression while the lower surface will be under tension.[33]

Consider a fiber at a distance from the neutral axis (N.A.). Because of the beam's curvature, the fiber is stretched by an amount of *cd*. Since the curvature of the beam is very small, *bcd* and *oba* are considered as similar triangles. The strain on this fiber is:

$$\epsilon = \frac{cd}{ab} = \frac{y}{\rho} \tag{A1}$$

A rod made of any elastic material can be viewed as a linear spring. It has length L and cross-sectional area A. Its extension (strain) is linearly proportional to its tensile stress σ, by a constant factor, the inverse of its modulus of elasticity, E. Hence,

$$\sigma = E\epsilon \tag{A2}$$

or

$$\Delta L = \frac{F}{EA}L = \frac{\sigma}{E}L \tag{A3}$$

By Hooke's law,

$$\epsilon = \frac{\sigma}{E} \tag{A4}$$

and

$$\frac{\sigma}{E} = \frac{y}{\rho} \tag{A5}$$

$$\sigma = \frac{y}{\rho} E \tag{A6}$$

which means that the stress is proportional to the distance y from the neutral axis. From this point on, f_b will be used instead of σ.

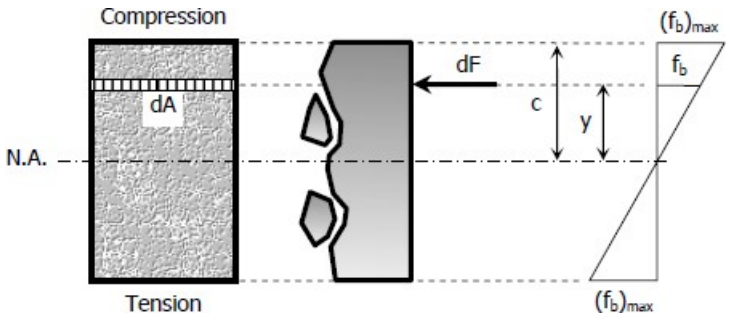

Figure A2: [33]

Considering a differential area $\mathrm{d}A$ at a distance y from the neutral axis, the force acting over the area is (see Figure A2):

$$\mathrm{d}F = f_b \, \mathrm{d}A = \frac{y}{\rho} E \, \mathrm{d}A = \frac{E}{\rho} y \, \mathrm{d}A \tag{A7}$$

The resultant of all the elemental moments about the neutral axis must be equal to the bending moment on the section.

$$M = \int \mathrm{d}M = \int y \, \mathrm{d}F = \int y(\frac{E}{\rho} y \, \mathrm{d}A) = \frac{E}{\rho} \int y^2 \, \mathrm{d}A \tag{A8}$$

Because

$$\int y^2 \, \mathrm{d}A = I \tag{A9}$$

$$M = \frac{EI}{\rho} \tag{A10}$$

or

$$\rho = \frac{EI}{M} \tag{A11}$$

Substituting

$$\rho = \frac{Ey}{f_b}, \tag{A12}$$

$$\frac{Ey}{f_b} = \frac{EI}{M}, \tag{A13}$$

$$f_b = \frac{My}{I} \tag{A14}$$

and

$$(f_b)_{max} = \frac{Mc}{I} \tag{A15}$$

The bending stress due to a beam's curvature is

$$(f_b) = \frac{Mc}{I} = \frac{\frac{EI}{\rho}c}{I} = \frac{Ec}{\rho} \tag{A16}$$

The beam curvature is:

$$k = \frac{1}{\rho} \tag{A17}$$

where

- ρ is the radius of curvature of the beam in mm (in)
- M is the bending moment in N·mm (lb·in) computed from the maximum load and the original moment arm
- f_b is the flexural stress in MPa (psi)
- I is the centroidal initial moment of inertia of the cross section about the neutral axis in mm^4 (in^4)
- c is the initial distance from the neutral axis to the extreme fiber where failure occurs in mm (in).

We now have the maximum tension, which occurs right as the beam breaks:

$$(f_b)_{max} = \frac{Mc}{I} \tag{A18}$$

The area moment of inertia of the cross section about the neutral axis is (see Figure A3)[34]:

$$(I_0) = \frac{bh^3}{12} \tag{A19}$$

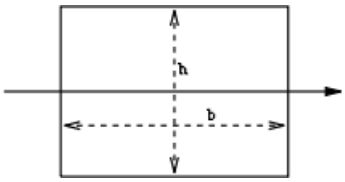

Figure A3: A filled rectangular area with a base width of b and height h.[34]

Because h = 2c,

$$(f_b)_{max} = \frac{Mc}{I} = \frac{M \cdot \frac{h}{2}}{\frac{bh^3}{12}} = \frac{6M}{bh^2} \tag{A20}$$

For a four point bending test, the load is applied through the inner span and reacted by the outer supports. For a load P, the reaction at one outer support is P/2, and the maximum moment produced is [35]:

$$\frac{P}{2} \cdot \frac{L-l}{2} \tag{A21}$$

Thus:

$$f_{b,max} = \frac{6}{bh^2}M = \frac{6}{bh^2} \cdot \frac{P}{2} \cdot \frac{(L-l)}{2} = \frac{3P(L-l)}{2bh^2} \tag{A22}$$

If a is the distance from one support beam to the closest load beam, then formula (A22) can be rewritten as:

$$f_{b,max} = \frac{3La}{bh^2} \text{ where } a = \frac{(L-l)}{2} \tag{A23}$$

The formula for the maximum fracture stress for the three-point bending test is similar to that of the four-point bending test. In formula (A22) we let l, the distance between the load beams, approach to zero:

$$f_{b,max} = \frac{3PL}{bh^2} \tag{A24}$$